THE ENGINEERS' DIGEST

REVIEW OF ENGINEERING PROGRESS ABROAD

VOLUME VIII.

JANUARY—DECEMBER, 1947.

Published by ENGINEERS' DIGEST LIMITED,
120 Wigmore Street, London, W.1.

The

ENGINEERS' DIGEST

REVIEW OF ENGINEERING PROGRESS ABROAD

VIII. No. 1 JANUARY, 1947

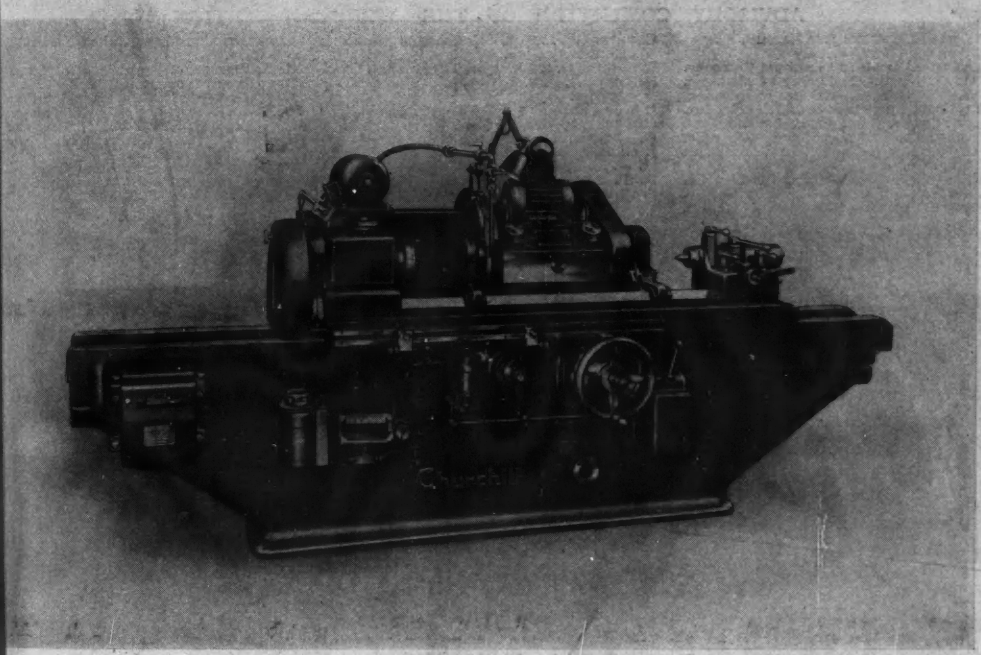

Churchill **PRECISION THREAD GRINDING MACHINES**
(with 'PULCRUSH' Equipment)

The most efficient application of the crushing method for the accurate and speedy grinding of all standard and special screw threads.

THE CHURCHILL MACHINE TOOL CO., LTD., MANCHESTER

HOME SELLING AGENTS: ---- Messrs. Chas. Churchill & Co., Ltd. (Birmingham and Branches)
EXPORT SALES ORGANIZATION: Associated British Machine Tool Makers Ltd. (London & Branches)

THE ENGINEERS' DIGEST

Published Monthly by Engineers' Digest Ltd., 120 Wigmore Street, London, W.1. Tel.: WELBECK

ANNUAL SUBSCRIPTION OF 12 NUMBERS, £2 2s. :: **SINGLE COPIES, 4s.**

ADVISORY COMMITTEE

J. F. ALCOCK, B.A., M.I.Mech.E.
R. W. ALLOTT, M.A., A.R.Ae.S.
E. ALTON, D.Eng., A.M.Inst.B.E.
R. W. AYERS, M.I.W.
Col. J. BOWDEN, M.Inst.C.E., M.I.Mech.E.
H. H. BROUGHTON, M.I.Mech.E.
F. BUCKINGHAM, B.Sc., A.M.Inst.C.E., A.M.I.Mech.E., A.M.I.E.E.
T. H. BURNHAM, B.Sc. (Lond.), A.M.I.Mech.E.
J. S. CASWELL, M.Sc., M.I.Mech.E.
G. C. SAFFERY COOPER.
J. DICK, Ph.D., B.Sc., A.M.I.Mech.E.
D. FIFE, M.I.Mech.E.
G. E. FOXWELL, D.Sc. (Lond.), F.Inst.P., F.Inst.F., M.Inst.Gas.E.
R. GRIFFITHS, M.Sc.
H. HEYWOOD, Ph.D., M.Sc. (Eng.), M.I.Mech.E.
O. HURST, M.Inst.N.A.
Capt. J. S. IRVING, M.I.Mech.E., M.I.A.E., A.F.R.Ae.S., M.S.A.E.
F. C. JOHANSEN, M.Sc. (Eng.), M.I.Mech.E., F.R.Ae.S., M.I.Loco.E.
W. J. KEARTON, D.Eng., M.I.Mech.E., A.M.Inst.N.A.
Prof. W. KERR, Ph.D., M.I.Mech.E.
G. V. LOMONOSOFF, Dr.Ing., M.I.Mech.E.
B. J. LYMER, M.I.Mech.E.
D. T. MACIVOR, M.I.Mech.E., M.Cons.E.
W. O. MANNING, F.R.Ae.S.
R. B. MATTHEWS, Wh.Ex., A.M.Inst.C.E., M.I.E.E., F.R.Ae.S.
Prof. A. L. MELLANBY, D.Sc., LL.D., M.I.Mech.E.
J. H. R. RATCLIFFE, B.Sc. (Eng., M.I.Mech.E.
Col. C. W. D. ROWE.
W. A. SCOBLE, D.Sc., A.R.C.Sc., M.I.M
P. W. SEBWER, D.E. (Zurich), M.Inst M.I.Mech.E.
Prof. S. PARKER SMITH, D.Sc., M. A.M.Inst.C.E.
C. E. H. VERITY, A.M.Inst.C.F., A.M. A.M.I.Mech.E.
E. G. WALKER, F.C.G.I., B.Sc. M.Inst.C.E., M.I.Mech.E., M.A.S
Major F. L. WATSON, M.I.C.E., M.I.M
G. WATSON, M.Inst.C.E., M.I.Mech.E.
C. H. WOODFIELD, M.I.Mech.E., M.I.St
T. WRIGHT, Ph.D., M.Sc.
M. L. YATES, Ph.D., M.Sc.Tech., M.A.(M.I.Mech.E.

ADVISORY COMMITTEE OF THE AMERICAN EDITION

Chairman: DR. ALEXANDER KLEMIN, New York University
R. S. ARCHER, Climax Molybdenum Company.
Prof. O. W. BOSTON, University of Michigan.
Dr. W. H. CARRIER, Carrier Corporation.
R. W. CARSON, Instrument Specialties Co., Inc.
Dr. L. W. CHUBB, Westinghouse Electric Corp.
A. E. RICHARD DE JONGE, Babcock & Wilcox Co.
Dr. O. S. DUFFENDACK, North American Phillips Co.
HANS ERNST, Cincinnati Milling Machine Co.
R. D. EVANS, The Goodyear Tire & Rubber Co.
CHRISTIAN E. GROSSER, Standard Machinery Co.
GEORGE F. HARACH, Worthington Pump & Machinery Corp.
Dr. VICTOR O. HOMERBERG, The Nitralloy Corp.
HERBERT R. ISENBURGER, St. John X-ray Service.
J. B. JOHNSON, A. A. F., Wright Field.
CHARLES M. JONES, John A. Roebling's Sons Co.
H. MANDEL, The Wickman Corp.
J. C. MATHES, Dow Chemical Co.
H. W. MCQUAID, Republic Steel Corp.
R. F. MILLER, Carnegie-Illinois Steel Corp.
Professor L. F. MOODY, Princeton University.
Professor H. F. MOORE, University of Illinois.
LAWRENCE OTTINGER, United States Pi Corp.
C. E. PRITCHARD, Republic Steel Corp.
JOHN SANDS, International Nickel Co.
JAMES G. SAWYER, Buffalo Turbine Corp
Dr. A. O. SCHMIDT, Kearney & Trecker
L. K. SILLCOX, New York Air Brake Co.
ALBERT F. SPERRY, President, Instr Society of America.
R. DAVID THOMAS, JR., Arcos Corp.
GEORGE A. TINNERMAN, Tinnerman Pr Inc.

Engin. Lib.
Bath.

REVIVAL OF GERMAN TECHNICAL LITERATURE

THE year which has just ended will probably go down in history as the turning point and certainly as the most important in the transition period from war to peace-time industry. There has been a remarkable change in all parts of the world by all concerned with industrial affairs in the outlook on life.

This change may not perhaps be apparent to the present generation who are so much preoccupied in dealing with the tribulations resulting from the war, but can be clearly recognized by professional observers accustomed to making more careful analyses.

At a recent Press Conference Sir Stafford Cripps, the President of the Board of Trade, stressed the importance of utilizing all sources of information available to find out the trend of technical and economic developments in these times of change-over. He particularly emphasized the value of the information gained from the results of practical experience and of the data of scientific research contained in the CIOS, BIOS, and FIAT Reports which have been prepared by some ten thousand investigators (industrialists, technicians and scientists) who visited Germany in about three thousand separate teams.

We were privileged to be included in these teams twice during the past year. Our visits were separated by an interval of seven months—May and December—and during our last visit we noted that an important change had taken place in the field of technical publications which will be of especial interest to our readers.

Whereas in the spring the leaves of trees and bushes camouflaged (albeit superficially) the raids on the devastated towns, no life seemed to be left in the erstwhile exuberant growth of the German technical press. Obviously, this impression was not quite correct ; a new start had already been made under the surface and whilst winter storm and frost pitilessly bared the deep wounds which the country had suffered, the first indications of a revival of German technical literature were seen.

We have now lying before us the first seven issues of a monthly periodical—" Die Technik " (July 1946 to January 1947). These have been published by the newly opened "Kammer der Technik" in Berlin and according to outward appearances this journal is the successor to the former well-known " VDI Zeitschrift."

Many articles are contained within the pages which we feel will be of interest to our readers to whom we hope to present abstracts in future issues of THE ENGINEERS' DIGEST. The following are characteristic examples of the contents of the seven issues :

H. UMSTÄTTER ; STRUCTURAL VISCOSITY IN RELATION TO LUBRICATING PROPERTIES.
E. GABER ; SAFETY OF STEEL BRIDGES.
H. VERSE ; INDUSTRIAL X-RAY EQUIPMENT.
W. BAUERSACHS AND P. GABLER ; INFLUENCE OF PRODUCTION UPON DESIGN IN LIGHT ENGINEERING.
H. FISCHER ; RECOVERY OF VALUABLE MATERIAL BY MODERN METHODS OF SURFACE TREATMENT.
A. SIEBEL AND S. SCHWAIGER ; PRESSURE VESSELS FOR THE CHEMICAL INDUSTRY.
H. UMSTÄTTER ; RHEOLOGY AND FLOW MECHANICS.
H. JUNGE ; PRESENT STATUS AND FUTURE DEVELOPMENTS IN HEAT ECONOMY.
B. HERMANN ; INCREASE IN EFFICIENCY OF EXISTING STEAM RAISING PLANT.
K. BAMMERT AND G. KORBACHER ; CHARACTERISTICS OF SINGLE-STAGE REACTION TURBINES.
K. H. KYSER ; COMPUTATION OF LOAD DISTRIBUTION IN TRANSFORMERS IN PARALLEL.
K. BLUME AND M. TETTENBORN ; THE KRUPP-RENN PROCESS.
P. LEINWEBER ; MEASUREMENTS IN THE WORKSHOP.
G. MARX ; WORKING CYCLES OF INTERNAL COMBUSTION ENGINES.
H. SCHROPP ; INFLUENCE OF IRON IMPURITIES AND OF ALLOYING ELEMENTS UPON THE QUALITY OF STEEL.
O. FÖPPL ; APPROXIMATE GRAPHICAL COMPUTATION OF TORSIONAL VIBRATIONS AND CRITICAL SPEEDS.

Although these journals are out of print, we succeeded in obtaining either copies or page proofs from which to make our abstracts.

The publication of " Die Technik " is not the only sign of revival in German technical literature, as we discovered during our recent visit. The following list of journals already published, or in course of preparation, certainly indicates that the revival of this important branch of industrial information surveys has begun again from many different angles.

ARCHIV FÜR METALLKUNDE	METALLFORSCHUNG
CHEMISCHES ZENTRALBLATT	NATUR UND TECHNIK
GLASERS ANNALEN	STAHL UND EISEN
KUNSTSTOFFE	WERKSTATT UND BETRIEB

Thus, in our special range of work, we may be entitled to say that the advice which Mr. Hynd, the Minister responsible for the Civil Government of the British Zone in Germany, gave in his Christmas message from London and Hamburg, had already been put into practice and which may be summarised by Carlyle's philosophy " Work and do not despair."

In a similar degree we, too, will push on with our work in these unsettled days, and hope that our readers will soon be able to surmount the difficulties which lie ahead, with the firm conviction that the year 1947 will be a step still further forward in the construction of a settled peace economy.

With all the compliments of the season we wish all our readers and friends a happy and prosperous New Year.

THE EDITOR.

FRANCE

WELDED CONSTRUCTION OF A DROP-SHAPED CONTAINER FOR LIQUID FUEL

(From *Le Génie Civil*, Vol. 123, No. 21, November 1, 1946, pp. 298, 3 illustrations.)

A NEW type container for liquid fuels has been designed by A. Caquot and erected at the " Amilly " Depot of the French Army Ordnance Services.

Similar to the new American spherical and ellipsoidal reservoirs[1], this new container has a surface of revolution, in this case that of a drop of liquid resting upon a horizontal surface. The curvature of the walls, however, has been calculated to take account of contributory factors such as capillary tension of the liquid, vapour pressure exerted on walls and liquid, changing liquid level, and plate buckling due to vertical and horizontal constraint of the plates. The ideal form for a gas container would be a sphere, for a liquid container a pure drop form if it were not for the danger of plate buckling. In U.S.A., this danger is countered by interior bracing which divides the plates into small free areas and is therefore very complicated. In the " Caquot " container bracing is dispensed with by addition of a supported cylindrical girdle CD (Fig. 1) at the plane of maximum diameter. The walls above and below this girdle are left free to expand and conserve the continuity and optimum drop form of the reservoir.

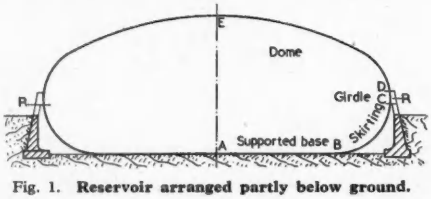

Fig. 1. **Reservoir arranged partly below ground.**

Actually the girdle serves to support a considerable part of the downward tension load exerted by the liquid on the skirting BC and to resist the upward tension load exerted by vapour pressure on the dome DE. The radii of curvature are determined by these effects. The deflection of the girdle at any point C of its circumference results from the vertical and horizontal thermal expansion and follows a radial direction AC, where A is the base centre.

Up to now, the spheroidal form has hardly been used for hydrocarbon reservoirs because designers have relied on construction methods employing wooden frame structures of single curvature and because double curvature calculations are difficult and differ considerably from normal strength of material calculations. Moreover, experiments with and tests of these container forms are complicated, and quality of design has therefore to be relied upon. Designers have been reluctant to develop large scale reservoirs and the main problem has been to find a simple method of calculation[2].

If, as shown in Figs. 1 and 3, the girdle is attached to brickwork, the rollers or flexible support pillars R are arranged vertically to a straight line AC. The girdle must be rigid enough to resist deformation of the reservoir and is stiffened by a bandage of reinforced concrete (Fig. 3). With these provisions, the constraint of the plates is only weak and the plates can be made relatively thin. The material need not be high tensile steel, but can be a corrosion resisting, easily deformable and weldable steel. At Amilly, a low carbon Martin steel was chosen (U.T.S. 22 to 28 tons, elongation 22 to 28 per cent) for plate thicknesses of $\frac{3}{16}$ to $\frac{4}{16}$ in. (Fig. 2). This reservoir has a capacity of 123,000 cub. ft., its height is 44 ft. 7 ins., its girdle diameter 70 ft. 5 ins., its base diameter 45 ft. 7 ins., and the radius of curvature varies from 9 ft. 8 ins. at B (Fig. 1) to 35 ft. 2 ins. at E.

The construction of the reservoir was fairly simple (no bracing required), took only six weeks and was finished by Nov. 1st, 1945. The plates for base and dome were arc welded, those of the girdle oxy-acetylene welded, two, three or four plates always forming one shaped panel unit. These panels were butt welded on site. For ease of assembly, the dome was built up in three parts, and the circumferential joints of base, skirting, girdle and dome rings were lap welded as shown in Fig. 2. For assembly at site, Mr. Tesson developed a jig structure (Fig. 3) consisting of a central lattice column, two opposite horizontal arms which turn round the central pillar and carry articulated and balanced fore-arms with welding cradles for welders and welding tackle. The welders operate motor winches for vertical movement of the cradles and hand winches for horizontal movement of the arms.

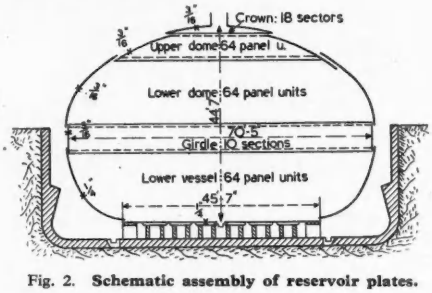

Fig. 2. **Schematic assembly of reservoir plates.**

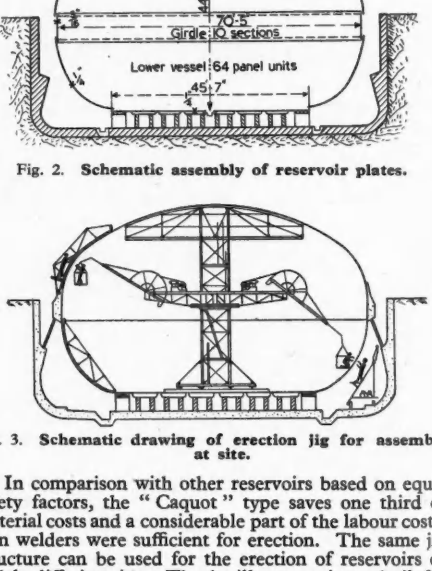

Fig. 3. **Schematic drawing of erection jig for assembly at site.**

In comparison with other reservoirs based on equal safety factors, the " Caquot " type saves one third of material costs and a considerable part of the labour costs. Ten welders were sufficient for erection. The same jig structure can be used for the erection of reservoirs of widely differing sizes. The Amilly reservoir was built for a vapour pressure of 20·5 lb./sq. in. abs. Correctness of shape and elastic deformations were first checked under air pressure of 22 lb./sq. in. abs. Several leaks were discovered and repaired. The official specification asked for a water pressure test at 26·3 lb./sq. in. abs., for repeated tests for air tightness and for measurement of temperature variations inside the reservoir.

The " Caquot " type reservoir can also be used for containers erected completely above ground, the girdle then being supported by pillars, and for containers with domes protected by external reinforced concrete caps.

BIBLIOGRAPHY.

(1) *Le Génie Civil*, 21-10-39.
(2) J. SOULASSOL, Moniteur des Travaux Publics et du Bâtiment, 1-6-1946.

NEW DEVELOPMENT IN THE DESIGN OF HIGH SPEED TURBO-ALTERNATORS

By A. MÁNDI. (From *Elektrotechnika*, Vol. 38, No. 1-6, May 1, 1946, pp. 6-16, 18 illustrations.)

ROTOR CONSTRUCTIONS.

ON account of the high peripheral speeds, the design problems of large capacity turbo-alternators turn upon the rotor, rather than the stator, the former being in fact the "soul" of the machine. The main rotor problems to be dealt with are mechanical stresses caused by the centrifugal forces, the winding and its securing, and finally the cooling.

Two fundamentally different rotor types have been developed, i.e. the radial-slot and the parallel-slot types.

In the radial-slot type rotor there are two methods of forming the slots. They can be milled in the main rotor body (Fig. 1a) or formed outside the main core by inserted teeth (Fig. 1b). With the milled slot type the flat strap conductors have to be dropped into the slots one at a time, with insulation between individual turns, whereas with the inserted-tooth type the coils can be assembled and insulated (Fig. 1c) before being fitted to the core. Both types of coils are of double curvature, neither of them can therefore be wound under stress. Due to uneven linear expansion of the coils and the rotor body, caused by a different temperature rise, a relative longitudinal movement of the two parts ensues which results in a slow deterioration of the coil-insulation and eventually in a break-down of the rotor. The end-connections overhang the core and require outside support which consist of non-magnetic steel caps (Fig. 1e) or binding wire. As a consequence of its longitudinal movement the end-winding—in the case of very long rotors—has to be supported on its inside by a special slidable part. These arrangements have set some of the most difficult problems with this type of construction. Main body and shaft-ends usually constitute one forged piece (Fig. 1f).

The *inherent advantage of the radial-slot rotor* is that there are no bending stresses in the teeth (Fig. 4d); this rotor type therefore allows maximum possible utilization as regards the total built-in copper section, resulting in maximum possible machine output for given dimensions of the rotor body.

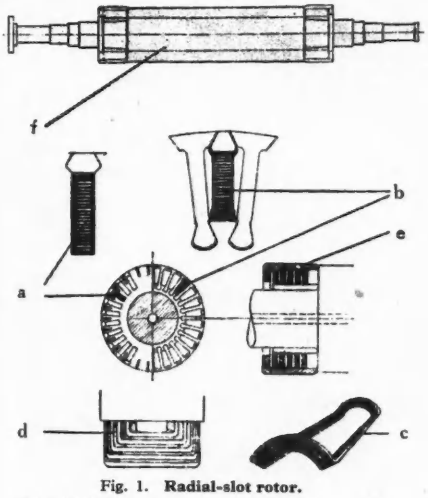

Fig. 1. **Radial-slot rotor.**

(*a*) milled-slot type
(*b*) inserted-tooth type
(*c*) coil
(*d*) end connections
(*e*) end shield
(*f*) complete rotor

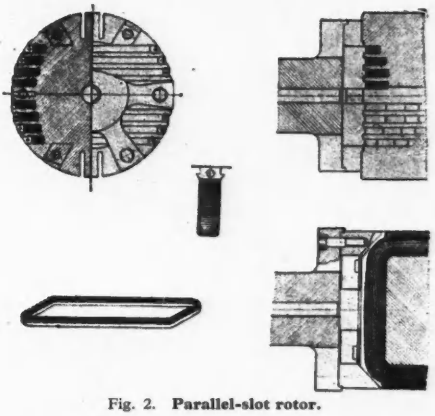

Fig. 2. **Parallel-slot rotor.**

Whereas nearly all electrical firms adhere to the radial-slot design, *Ganz & Co.* (Budapest, Hungary) have chosen the *parallel-slot rotor* at the very beginning of their manufacture of high speed turbo-alternators and kept to this design ever since, developing it to a very high degree of perfection.

In the parallel-slot type rotor the slots are milled, not only in the sides of the main body, but also across its ends, so that the coils are embedded in the metal throughout the whole of their length (Figs. 2 and 3).

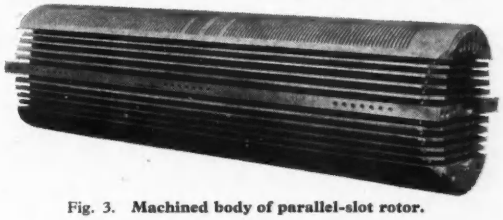

Fig. 3. **Machined body of parallel-slot rotor.**

The advantages of the parallel-slot rotor are: As the coils are secured by the core throughout the whole of their length against the action of the centrifugal force, no shields or bending wire have to be used, nor are packing pieces required.

All the coils—consisting of hard-drawn flat wound copper strips—are tightly wound under stress, the mica-insulation between the turns being inserted at the same time. The stress applied during winding causes a greater elongation of the copper strip than that effected by the heat. Therefore the temperature rise only decreases the effect of pre-stressing, but no relative longitudinal movement between copper and steel obtains. The mechanical method of winding makes it possible to apply constant pressure and to make the coils so hard that, when finished, they give a metallic ring and constitute a very compact component.

The coils are wound in the slots with 0·1 mm. negative tolerance (the straps are 0·1 mm. broader than the inner width of the slot-insulation); no air remains between tooth, mica and copper. In the course of winding, each coil is heated several times up to 150-160 deg. C., so that the excess binding material of the mica is pressed out, and the copper, the insulation and the

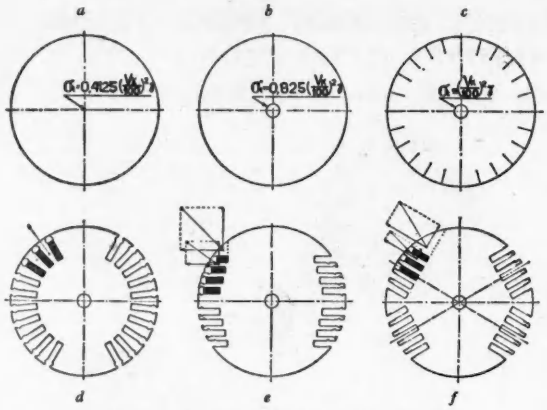

Fig. 4. **Stresses caused by the centrifugal force.**

(*a*) full main rotor body
(*b*) bored „ „ „
(*c*) bored and cut-in main rotor body
(*d*) radial-slot rotor
(*e*) parallel „ „
(*f*) crossed-coil „

steel becomes one solid body, in which no air is trapped. The coils are insulated along their whole length, and also between turns, with pure hard mica.

The rotor coils are covered by a steel strip binding, enclosing completely the copper as well as the insulating material ; in this rotor, steel only is visible and accessible. The insulating material is out of the reach of fire.

The rotor is heat-resisting to a very high degree. An alternator of the type dealt with has been running for several hours in single-phase short-circuit. The rotor temperature reached abt. 300 deg. C. without its insulating qualities being affected in any way.

A rotor of this design was submitted to temperatures of 200 to 300 deg. C. during 120 hours at the normal speed of 3000 r.p.m. Insulation and balance remained perfect. A breakdown of this " steel-clad " rotor is practically impossible.

The two end-shafts are bolted to the core by means of flanges ; the forged body is therefore far shorter than in the case of the radial-slot rotors.

The inherent backward of the parallel-slot rotor is that all the teeth are submitted not only to longitudinal stresses but also to bending moments which are partially transmitted to the adjacent tooth. The sum of these moments acts on the nose-shaped tooth at the centre (Fig. 4e) resulting in a design-limiting stress ; therefore the total slot and copper sections are smaller than is possible with radial-slot rotors of equal diameter, i.e. with equal rotor dimensions and material, the possible machine output is reduced. The bending stress in the teeth sets a limit to the rotor diameter at a value lower than that permissible with radial-slot rotors where the diameter is only limited by the stress in the body itself.

THE CROSSED-COIL ROTOR.

In order to eliminate the only drawback of the parallel-slot rotor *Ganz & Co.*, have, in the course of recent years, developed a new rotor construction. It keeps all the advantages of the parallel-slot system but, by decreasing materially the mechanical stresses in the teeth, permits a better utilization. With equal rotor main dimensions and using the same material, the total copper section and machine output is increased considerably as compared with the simple parallel-slot construction.

This new type, the crossed-coil rotor,* contains two separate parallel-slot systems crossing each other under a certain angle at the frontal part of the rotor body. When dealing with the original parallel-slot rotor we have seen that, the farther we go from the axis of symmetry of the system (Fig. 4e) the greater is the increase in the bending stress in the teeth and the smaller the slot area available for the winding. With the new type of rotor (Fig. 4f) only the slots near the axes of symmetry of each slot-system are used and since no room for bolt-holes is required, even the two axes of symmetry can be utilized. On account of this slot-arrangement, the bending component of the centrifugal force (perpendicular to the length of the teeth) and therefore also the bending stress in the teeth, becomes relatively small and the stresses in the teeth are nearly exclusively of a tensile character. The mechanical stress of the nose-shaped tooth is far smaller than it is in the case of the original parallel-slot rotor. This is due partly to the fact that the bending component acting on this tooth is much smaller and partly to its much larger root-width. As a consequence of these circumstances, this tooth ceases to be the weakest part of the rotor design.

Let us now consider the solution of the most difficult constructional problem presented by the new rotor type, viz. : that of the frontal crossing of the two coil systems.

The front parts of the inner coil system are lying in slots of the main rotor body (Figs. 5a and 6a) just as in the case of the original parallel-slot rotor. After complete winding and wedging of the inner coils a cover piece (Figs. 5f and 7) is placed at the front-ends of the

* The author's design, patent claim filed.

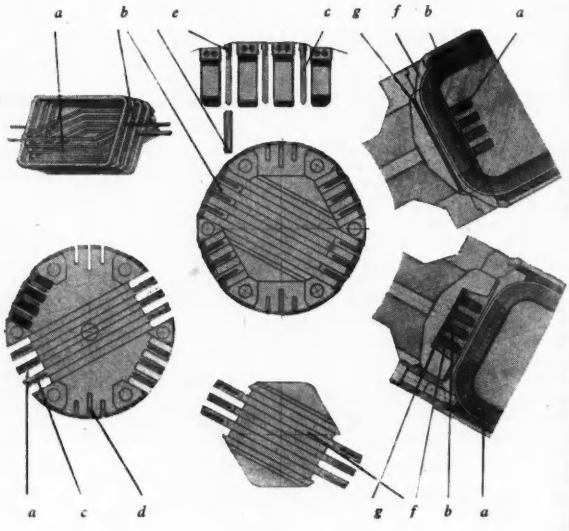

Fig. 5. **Crossed-coil rotor.**

(*a*) inner coil system
(*b*) outer „ „
(*c*) ventilating ducts in the teeth
(*d*) ventilating ducts in the poles
(*e*) closing wedge of ventilating duct
(*f*) cover piece
(*g*) covering plate.

rotor body. This cover contains the milled continuations of the longitudinal slots and the frontal slots of the second coil system, crossing the frontal slots of the first (inner) coil system. After placing and fixing these cover pieces the outer coil-system can be wound and wedged. Finally, to secure the teeth of the cover piece against opening by the bending effect of the centrifugal force, a flanged cover-plate (Fig. 5g) is placed at each end of the rotor body. The flanged shafts are attached by means of six bolts, two of which can be placed between the two slot systems. The constructional parts of the coil-crossing do not increase appreciatively the length of the rotor, as the latter has protruding arms even in the case of the original parallel-slot rotor.

The advantageous stress conditions permit arranging ventilating ducts in the teeth (Fig. 5 and 6c). In order to prevent a considerable weakening of the thin rotor teeth, it is advisable to provide the wedges fixing the coils with multiple teeth, having a small circumferential dimension.

Fig. 6. **Machined body of crossed-coil rotor.**
(*a*) slots of the inner coil system
(*b*) „ „ „ outer „ „
(*c*) ventilating ducts in the teeth
(*d*) „ „ „ „ poles.

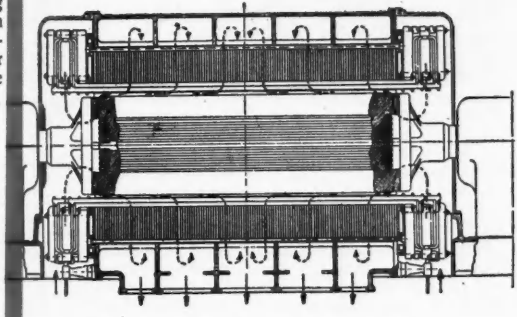

Fig. 9. **Stator ventilated through the air-gap.**

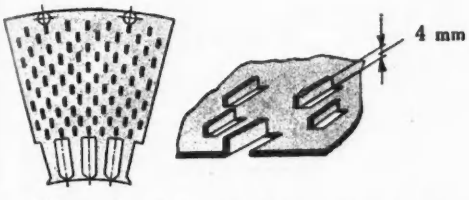

Fig. 10. **Outer laminations acting as distance pieces.**

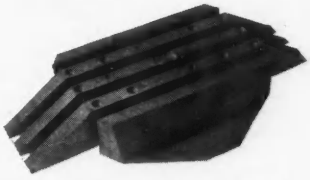

Fig. 7. **Cover piece.**

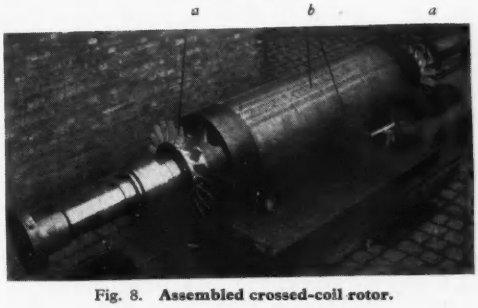

Fig. 8. **Assembled crossed-coil rotor.**
(*a*) axial fans (*b*) outlet ducts.

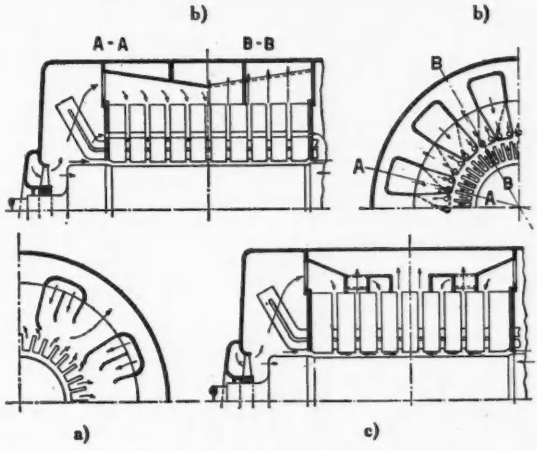

Fig. 11. **Separate stator cooling.**
(*a*) inlet and escape through the same duct
(*b*) „ „ „ „ different duct-groups by way of axial passages
(*c*) „ „ „ „ the same ducts by way of the air-gap.

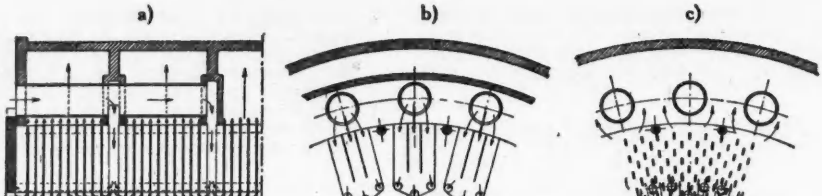

Fig. 12. **Separate stator cooling with special outer ducts.**
(*a*) longitudinal section
(*b*) cross section through inlet ducts
(*c*) „ „ „ outlet ducts.

To ensure sound execution of this design, the teeth have to be fitted into the wedge-slots with considerable pressure. In order to fulfil these requirements the wedges are milled with the same tool as the wedge-slots. The wedges closing the ventilating ducts are each made of two parts (Fig. 5e); after winding the coils and fitting the slot wedges, the wedges of the ventilating ducts are inserted and very firmly secured.

Ventilating ducts can be arranged also in the poles of the rotor body (Figs. 5 and 6d). The cooling air entering the alternator at both ends leaves the rotor through ducts in the centre part of the rotor body (Fig. 8b).

The insulation, coils and fixing details of the crossed-coil rotor are practically the same as in the case of the simple parallel-slot rotor, and therefore its main advantages are also similar, i.e. the coils are in one plane and can therefore be wound under stress and pressure. Heat resistance is high, the insulation compact, and no air is trapped in the windings which are steel-clad.

Special advantages attached to the cross-coil design are: (*a*) Considerable increase in the total copper section and therefore far better utilization of the material. Experience shows that with equal main rotor dimensions 25 to 40 per cent larger output is obtainable as compared with the original parallel-slot rotor design. (*b*) since bending stresses in the teeth are smaller, they no longer set a limit to the rotor diameter, the value of this latter being limited—as in the case of the radial-slot rotor—only by stresses in the rotor body itself. The machine capacity obtainable with ordinary Siemens-Martin steel is increased from a former 20,000 to about 50,000 kVA. Only above this value the use of alloyed steel (chrome-nickel-molybdenum) is necessary.

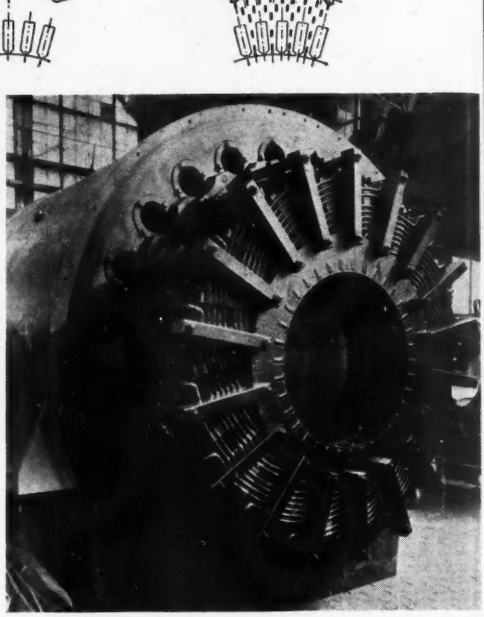

Fig. 13. **Assembled stator with cooling system according to Fig. 12.**

Although the maximum copper section with the crossed-coil rotor is still slightly smaller than with the radial-slot rotor, this is compensated for by the better heat-conducting and heat-resisting qualities of the crossed-coil rotor and consequently, with given main rotor dimensions, the same output is obtainable in both cases.

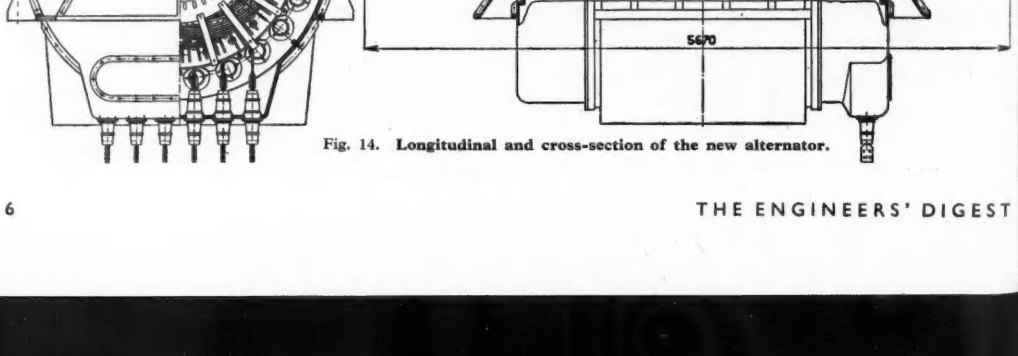

Fig. 14. **Longitudinal and cross-section of the new alternator.**

STATOR DESIGN AND COOLING.

The simplest ventilating system is shown in Fig. 9, which also shows the path of the cooling air. A drawback to this design is the comparatively small area of the air-gap, thus limiting the circulation; an advantage is that a comparatively large number of ventilating ducts can be arranged in the stator by dispensing with separate ventilating disks the height of which is at least about 10 mm. for 50 mm. core stacks. The outer laminations of a 20 mm. stack can be so shaped as to act as distance pieces, their height being 4 mm. (see Fig. 10). The temperature rise inside the core stacks is—in consequence of their small axial dimension—also very small.

Other designs are shown on Fig. 11; the air paths are clearly indicated. These cooling systems may also be combined; their advantages are: larger sections for the passing air, smaller air velocities and windage losses even with large air quantities; and their disadvantages: 10 mm. high distance pieces, smaller number of ducts and higher temperature rise inside each stack. Owing to the considerably larger air quantities, the total temperature rise is (mainly in the case of comparatively long machines) less than with the cooling system shown in Fig. 9.

The cooling system adopted by *Ganz & Co.* for the stators of the machines with crossed-coil rotors aims to unite the advantages of the designs shown on Figs. 9 and 11. In the design shown in Fig. 12, one part of the air delivered by the axial fans enters the air gap and the rotor ducts, while the other part, passing the end-windings, gets into axial tubes arranged outside the stator core which end in U-shaped pockets in the stator frame (Fig. 12a). The stator core is provided with a few wide and deep entrance pockets (Fig. 12b) connected by axial passages to a large number of 4 mm. wide air ducts (Fig. 12c). The air coming from the axial tubes is passed through the wide ducts, from these into the narrow ones and, joining in the latter, the air coming from the air gap, leaves the stator core at its outer circumference (Fig. 12c). This system unites the advantages of large air quantity with that of large cooling surface. The assembled stator is shown in Fig. 13, the sections of the alternator in Fig. 14.

Quite a number of alternators have been built with crossed-coil rotors incorporating the new cooling system, all with rotors of Siemens-Martin steel. The largest capacity is 44,000 kVA. The first rotor of the new design has been tested for 2 minutes at 4000 r.p.m to prove its reliability; no defect could be detected on the rotor after testing, the balance remaining perfect. Output and temperature rise on test have been in full accordance with calculated values. The new design has therefore fulfilled all expectations.

FRANCE

INFLUENCE OF WATER INERTIA ON THE STABILITY OF OPERATION OF A HYDRO-ELECTRIC SYSTEM

By P. ALMÉRAS. (From *La Houille Blanche*, Nos. 1, 2, 3, November, 1945/January, 1946, March, 1946, May, 1946, pp. 81-90, 131-139, 189-198, 14 illustrations.)

A GOVERNOR must show two essential qualities, quick response and stable control. In an ideal system, the power generated should, at any moment, be equal to the power required. This cannot be attained in practice as the governors of the generating machinery only detect a change of load after a certain parameter has changed, and the best they can do is to attain, as quickly as possible, a new equilibrium. Normally, the parameter is the electric frequency, its change causing a change of generator (or motor) speed, and is detected by a simple fly-ball governor. The governor only runs in equilibrium (constant speed) if the inlet port opening of the machine has certain value corresponding to the governor speed. Fig. 6 represents this, normally linear, relationship, with the ratio of actual to normal working speed as ordinate and the degree of inlet port opening as abscissa. When load changes demand it, the governor should transfer the control point from one point of the curve to another with the least possible deviation from the curve itself. As the load, and therefore the frequency can change very suddenly, the governor must respond quickly in order to minimize these deviations, i.e. the centrifugal governor must be sensitive, and the control relays very quick. This is one of the reasons why some designers add to the speed governor action an acceleration governor (rate of speed change controller) which acts from the very first start of a disturbance.

A quickly responding governor may however overshoot the point of new equilibrium, then reverse its movement, overshoot again and reach the new equilibrium only after many oscillations. This is inadmissible and a system is considered stable only if these oscillations are damped out very quickly.

If several systems are interconnected, it is the stability of the interconnecting lines that matters. The French electricity net-work has a great stability margin so that, under favourable conditions, several inherently unstable groups can be connected to it and still leave it stable as a whole if the interconnecting lines have suitable characteristics.

NOTATION.

t = time

ω = speed at time t

$x = \frac{\omega}{\omega_0}$ = relative speed at time t

ω_0 = normal working speed

H = effective head at time t

H_0 = normal static head

$\Delta h = H - H_0$ = rise of head due to water hammer

$\zeta = \frac{\Delta H}{H_0}$ = total relative pressure rise (comprising upstream rise plus downstream pressure drop.

R = opening position of gate (or guide vanes or nozzle control) at time t, expressed in discharge quantity under head H_0

R_0 = gate opening corresponding to the required power output

R_p = full gate opening (maximum discharge quantity under head H_0)

P = output of system at time t and under gate opening R

P_0 = output required by net (load)

P_p = output at full gate opening R_p under head H_0

Q = discharge at time t

Q_p = discharge at full gate opening under head H_0

$y = \frac{R}{R_p}$ = relative gate opening at time t

$y_0 = \frac{P_0}{P_p} = \frac{R_0}{R_p}$ = relative gate opening corresponding to load P_0, under head H_0

σ = stabilization degree

K_0 = speed of response of tachometric governor

K_1 = speed of response of accelerometric controller

ω' = speed aimed at by tachometric governor at time t

$\tau = \frac{\mathcal{J}\omega_0^2}{P_p}$ = time taken to start up machinery from zero to working speed, with fully open gates

L = total penstock length plus half developed length of spiral intake plus length of draft tube

V_i = water speed in different successive parts of penstock, intake, draft tube, at gate opening y

V_{ip} = Do. at full gate opening $y = 1$

$V = \frac{\Sigma L_i V_i}{L}$ = mean effective water speed at time t

$V_p = \frac{\Sigma L_i V_{ip}}{L}$ = mean effective water speed at full gate opening under head H_0

$\Theta = \frac{LV_p}{gH_0}$ = characteristic time-constant of conduit

$\mathcal{J}$ = moment of inertia of system

A. THE CASE OF A SYSTEM FEEDING A SEPARATE INDEPENDENT NET.

The governor detects a change of load by variations of speed in the tachometric governor (and of acceleration in the accelerometric controller if fitted) and then acts so as to equalize output with loading. If the governor has no rigid restoration, then the new speed, and consequently the new frequency, are equal to the previous ones. A stable system will reach the new equilibrium aperiodically or by rapidly damped oscillations. Actually, damping is normally so strong that only the first oscillation is noticeable and the new equilibrium is reached at the beginning of the second oscillation.

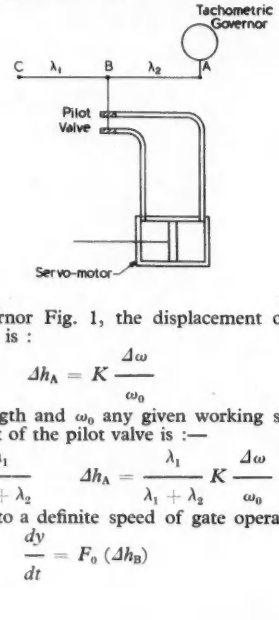

Fig. 1.

I. DEFINITIONS.

For the governor Fig. 1, the displacement of the tachometer sleeve is :

$$\Delta h_A = K \frac{\Delta\omega}{\omega_0}$$

where K is a length and ω_0 any given working speed. The displacement of the pilot valve is :—

$$\Delta h_B = \frac{\lambda_1}{\lambda_1 + \lambda_2} \qquad \Delta h_A = \frac{\lambda_1}{\lambda_1 + \lambda_2} K \frac{\Delta\omega}{\omega_0}$$

Δh_B corresponds to a definite speed of gate operation :

$$\frac{dy}{dt} = F_0(\Delta h_B)$$

where y is the relative gate opening position, $0 < y < 1$. F_0 is the response function of the pilot valve and depends on gate (or vane or nozzle) opening position, mainly because the effort required to open the guide vanes is different for different vane positions, and also because the degree of opening, expressed in terms of discharge quantity, is not proportional to the servo-motor displacement. The gate speed reaches a maximum after a definite valve displacement Δh_B (saturation point of distributing mechanism, see Fig. 2). For small displacements and neglecting any elastic recovery of the linkage, the function is practically linear. Therefore :

$$\frac{dy}{dt} = -K'\Delta h_B = -KK' \frac{\lambda_1}{\lambda_1 + \lambda_2} \frac{\Delta\omega}{\omega_0} = -K_0 \frac{\Delta\omega}{\omega_0}$$

If the tachometric governor is replaced by an accelerometric controller, the accelerometric response for small displacements would be :

$$\frac{dy}{dt} = -K_1 \frac{d}{dt} \frac{\Delta\omega}{\omega_0}$$

K_0 and K_1 are the " response speeds " of tachometric governor and accelerometric controller. If backlash and friction in the governing linkage are considered, Fig. 2 changes to Fig. 3, with two curves separated by the distance $2i$, where i represents the amount of sluggishness in the governor. If speed or acceleration oscillate between A and A', then the point representing the gate operating speed describes the cycle shown in Fig. 3.

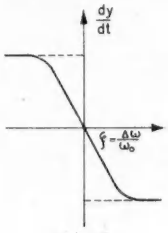

Fig. 2.

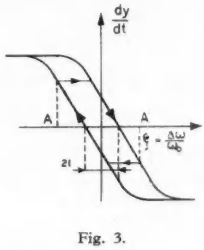

Fig. 3.

The governor Fig. 1 is unstable, even if infinitely sensitive or if water inertia is neglected. A restoring or relay mechanism (Fig. 4) or an accelerometric governor (Fig. 5) must be added. Fig. 4 shows that equilibrium of the pilot valve (no oil being supplied to servo-motor) is possible for different governor sleeve positions, hence for different governor speeds, depending on servo-motor (gate opening) position. After a disturbance has taken place, the governor therefore aims at attaining a new speed depending on the gate opening position. The restoring cam (Fig. 4) is such that to each gate position y (expressed as discharge under constant head H_0) corresponds a definite height h_C of point C, $h_C = \phi(y)$.

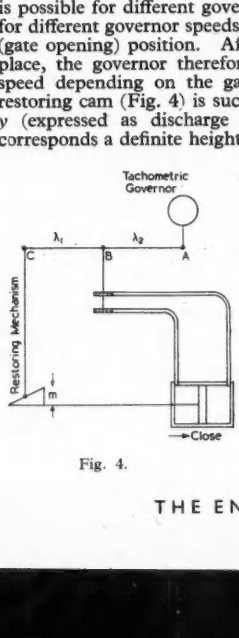

Fig. 4.

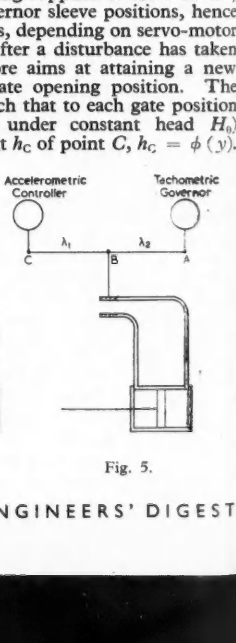

Fig. 5.

For a definite opening, the slope $\frac{dh_C}{dy} = m$. For rectilinear cam and y proportional to servo-motor displacement, m is the cam slope or total height of the cam (Fig. 4).

Therefore :

$$\Delta h_B = \frac{\lambda_2}{\lambda_1 + \lambda_2} \Delta h_C + \frac{\lambda_1}{\lambda_1 + \lambda_2} \Delta h_A$$

and, using the preceding equations,

$$\frac{dy}{dt} = -K_0 \left[\frac{\omega - \omega_0}{\omega_0} + \sigma (y - y_0) \right] \qquad (1)$$

where $$\sigma = \frac{\lambda_2}{\lambda_1} \frac{m}{K} = \frac{\Delta \frac{\omega'}{\omega_0}}{\Delta y}$$

is the degree of restoration for gate opening y_0. ω' is the "aimed at" speed governor, a function of y, and given by :

$$\frac{\omega'}{\omega_0} = 1 - \sigma (y - y_0)$$

With accelerometric controller (Fig. 5), the corresponding equation is

$$\frac{dy}{dt} = -K_0 \frac{\omega - \omega_0}{\omega_0} - K_1 \frac{d \frac{\omega}{\omega_0}}{dt} \qquad (1')$$

Fig. 6 gives relative gate opening as abscissa and relative "aimed at" tachometric governor speed as ordinate. The restoration curve thus obtained is usually rectilinear.

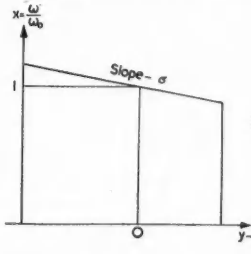

Fig. 6.

II. Generally known results.

Elementary theory shows that, neglecting water inertia and assuming stable water flow through the turbine and a perfectly designed governor, a small degree of restoration σ or a small positive accelerometric addition K_1/K_0 make a system stable. Critical conditions (undamped oscillations) are reached theoretically for $\sigma = 0$ or $K_1 = 0$ if by-effects of turbine or electric net-work are neglected. For stability of governing, the effects of a restoring mechanism or of an accelerometer are identical. However, every governor is somewhat insensitive, the servo-motor piston hunts slightly, and the relative amplitude of hunting, in terms of total gate travel, is of the order of i/σ, whatever the response speed of the governor with restoration. The governor, therefore, needs a greater degree of restoration the more imperfect its construction. Usually, a restoration degree of a few per cent is sufficient for well designed governors and this is weak enough to dispense with interposition of a dash-pot. For negligible water inertia and stable water flow, a weak and rigid restoration (which is always needed if several systems work in parallel) guarantees sufficient stability. A stronger restoration effect with dash-pot or accelerometric governor is only required where water inertia in closed conduits has to be considered or where water flow through the turbine is not stable (e.g. running on no load).

III. Effect of water inertia.

In most installations, when the turbine gates are commencing to close, water inertia creates an overpressure and produces a rise in output although the governor action tends to diminish it. The difficulty has been overcome by an increase in restoration effect, and/or by the addition of an accelerometric controller to the speed governor. For mathematical treatment, the following simplifying assumptions are made :—

(a) Accelerometric controller and tachometric governor have small inertia so that the sleeve position at any instant indicates the exact speed or acceleration of the system. Inertia would create a time lag unfavourable for governing stability. This is one reason for the reduction of masses in modern design. This assumption is justified for modern governors.

(b) Oil-pressure relays between governor sleeve and pilot valve have no time lag, i.e. they act like a rigid connection. Time lag is actually very small in modern apparatus.

(c) System efficiency to be constant for small variations of speed, static head and gate opening. For a given head, the output is then proportional to gate opening but independent of speed.

(d) Electric load to be purely resistive, with instantaneous tension regulation. The load is then also independent of speed. This assumption is very unfavourable for system stability.

If these assumptions were not realized, the coefficients of the stability equations would have to be modified. At partial loads, the rise in efficiency with gate opening would favour stability, the decrease in efficiency near full load would be unfavourable. Therefore, the assumption of constant efficiency in working position appears to be justified, in its effect on stability, under normal loads.

(e) Only small movements following a load change are considered so that response laws of tachometric and accelerometric governors can be assumed to be linear.

(f) Elasticity of water and conduit walls is neglected, water inertia is considered as a mass phenomenon only. This is justified for low and medium head plants with relatively short penstocks where the travelling time of a water wave in the penstock is short compared with the natural frequency of the plant. Water inertia thus expresses itself in the parameter $\Sigma L_i V_i$.

IV. Fundamental equations.

System feeding an independent net-work. Working conditions : y'_0, ω'_0, P'_0. At time $t = 0$, the load passes from P'_0 to P_0 with corresponding y_0 and ω_0. How do y and ω change during this transition ?

(a) *Turbine movement.*

At time t :

$$P - P_0 = \mathcal{J} \omega \frac{d\omega}{dt}$$

$$\text{or } \frac{P - P_0}{P_\nu} = \frac{\mathcal{J} \omega_0^2}{P_\nu} \times \frac{\frac{\omega}{\omega_0} d \frac{\omega}{\omega_0}}{dt} =$$

$$= \frac{R}{R_\nu} \left(\frac{H}{H_0} \right)^{\frac{3}{2}} - y_0$$

or with x, y, ζ (no dimensions) :

$$\tau \frac{xdx}{dt} = y\,(1 + \zeta)^{3/2} - y_0 \qquad (2)$$

(b) *Water hammer.*

The principle of conservation of linear momentum demands, for a given gate operation :—

$$\Delta H = -\frac{L}{g}\frac{dV}{dt} = -\frac{LV_p}{g} \times \frac{d}{dt}\frac{V}{V_p}$$

L comprises, on the average half the developed spiral intake length because some water filaments pass through the whole spiral length, others go direct from the distributor into the turbine. This is important for Kaplan plants with short, or no penstocks. Further :—

$$\zeta = \frac{\Delta H}{H_0} = -\Theta \frac{d\,\frac{V}{V_p}}{dt} = -\Theta \frac{d\,\frac{Q}{Q_p}}{dt}$$

$$\frac{Q}{Q_p} = \frac{R}{R_p}\left(\frac{H}{H_0}\right)^{\frac{1}{2}} = y\,(1 + \zeta)^{\frac{1}{2}}$$

$$\zeta = -\Theta\left[(1 + \zeta)^{\frac{1}{2}}\frac{dy}{dt} + \frac{y}{2(1 + \zeta)^{\frac{1}{2}}}\frac{d\zeta}{dt}\right] \qquad (3)$$

(c) *Governor response laws.*

Equation (1) becomes :

$$\frac{dy}{dt} = -K_0\,[(x - 1) + \sigma\,(y - y_0)] \qquad (4)$$

Equation (1′) becomes :

$$\frac{dy}{dt} = -K_0\,(x - 1) - K_1\frac{dx}{dt} \qquad (4')$$

Assuming small movements and linear relationships, these equations 2, 3, 4, 4′ can be established as linear, homogeneous differential equations of the first order with constant coefficients. Taking $x = 1 + \xi$, $y = y_0 + \epsilon$, $\zeta = \zeta$, where ξ, ϵ, ζ are small quantities. Their squares, products with each other and each other's derivatives can be neglected. Therefore, finally the characteristic system equations are :

$$\frac{d\epsilon}{dt} = -K_0\,(\xi + \sigma\epsilon)$$

response law of stabilized tachometric governor,

$$\frac{d\epsilon}{dt} = -K_0\,\xi - K_1\frac{d\xi}{dt}$$

response law of accelero-tachometric governor,

$$\tau\frac{d\xi}{dt} = \epsilon + \frac{3}{2}y_0\,\zeta$$

turbine motion law,

$$\zeta = -\Theta\left(\frac{d\epsilon}{dt} + \frac{1}{2}y_0\frac{d\zeta}{dt}\right)$$

water inertia law.

V. GOVERNOR WITH RIGID RESTORATION.

Characteristic equations of system :

$$\left.\begin{aligned}\frac{d\epsilon}{dt} &= -K_0\,(\xi + \sigma\epsilon)\\ \tau\frac{d\xi}{dt} &= \epsilon + \frac{3}{2}y_0\,\zeta\\ \zeta &= -\Theta\left(\frac{d\epsilon}{dt} + \frac{1}{2}y_0\frac{d\zeta}{dt}\right)\end{aligned}\right\} \qquad (I)$$

Neglecting transmission time lags, this can be solved by putting :

$\epsilon = \lambda e^{rt}$, $\xi = \mu e^{rt}$, $\zeta = \nu e^{rt}$. (Assumptions (a) and (b).)

Then
$$\lambda\,(r + K_0\,\sigma) + K_0\,\mu + 0 = 0$$
$$\lambda - \tau r\mu + \frac{3}{2}y_0\,\nu = 0$$
$$\lambda\Theta r + 0 + \left(y_0\frac{\Theta r}{2} + 1\right)\nu = 0$$

If (and only if) the determinant is zero, the solution in λ, μ, ν can be written :

$$r^3 + r^2\frac{\tau\left(\frac{y_0\Theta K_0\sigma}{2} + 1\right)}{\frac{1}{2}y_0\Theta\tau} + r\frac{K_0(\tau\sigma - y_0\Theta)}{\frac{1}{2}y_0\Theta\tau} + \frac{K_0}{\frac{1}{2}y_0\Theta\tau} = 0$$

which has the general form : $r^3 + \alpha r^2 + \beta r + \gamma = 0$. The system is stable if the real parts of all the roots of this equation are negative, i.e. if, according to Hurwitz :

$$\alpha > 0,\ \gamma > 0,\ \alpha\beta - \gamma > 0.$$

If the third condition is fulfilled, the first two are automatically fufilled so that the final stability criterion is :

$$\frac{\tau\sigma}{y_0\Theta} > \frac{3 + y_0\Theta K_0\sigma}{2 + y_0\Theta K_0\sigma} \qquad (5)$$

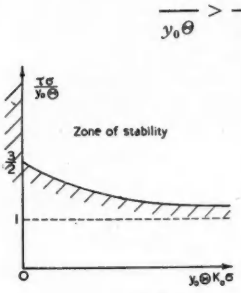

Fig. 7.

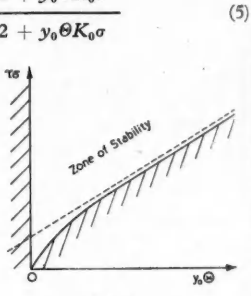

Fig. 8.

Equating the two sides would result in undamped vibrations of the system. Fig. 7 illustrates the criterion, Fig. 8 gives the same relationship for K_0 and σ constant and shows that for a given plant (Θ = const.), the critical minimum of τ grows with growing y_0, i.e. the criterion is more severe at full than at partial load. For full load, $y_0 = 1$, therefore $\frac{\tau\sigma}{\Theta} > \frac{3 + \Theta K_0\sigma}{2 + \Theta K_0\sigma}$.

$\tau\sigma$ and Θ play an important role in this criterion while $K_0\sigma$ is of secondary importance. Nevertheless, in order to diminish the value of the right side of the inequality, it is advisable to keep K_0 large, i.e. to use a governor with rapid response.

Putting $\tau > K\frac{\Theta}{\sigma}$, where $3/2 > K(K_0) > 1$, then choosing $K_{max} = 3/2$, and assuming further a medium head plant with $H = 120$ ft., $L = 300$ ft., $V = 12$ ft./sec., therefore $\Theta = 1$ sec., and a normal average starting-up time of $\tau = 7{\cdot}5$ sec., one would obtain $\sigma = 20$ per cent at the minimum. This would produce unacceptable frequency changes and the restoring mechanism therefore would have to be made elastic by interposition of a dash-pot. One must consider, however, how far elasticity reduces the stabilizing effect of the restoring mechanism.

(To be continued).

STEAM JET COMPRESSORS IN PROCESS STEAM PLANT

By A. A. KANAEV. (From *Vestnik Machinostroenya*, Vol. 26, No. 2/3, 1946, pp. 76-81, 10 illustrations.)

THIS article deals with various aspects of the employment of steam jet compressors in process steam plants with by-product power generation. The plant diagrams a, b, c, and d shown in Fig. 1 illustrate several representative examples of the use of steam compressors for the purpose of increasing the pressure of steam supplied for process purposes.

In the diagram (a) the steam jet compressor serves to re-compress the steam generated in the concentrator of a tomato canning factory. Similar arrangements are used in plants for the production of evaporated milk, and in various chemical processes. The diagrams (b) and (c) show steam compressor installations for increasing the pressure of the exhaust of back pressure turbines. In the plant represented by diagram (c2) the steam jet compressor serves to mix the live steam supplied by two boilers operating at different pressures, the steam delivered by the steam jet compressor having a higher pressure than that of the low pressure boiler. Diagram (d) shows a plant in which the steam compressed by the steam jet compressor is subsequently reduced to the requisite process temperature by means of a spray type desuperheater.

Diagram (e) shows a circuit of the type mainly used in combined heat and power plants. A certain amount of the exhaust steam of one back pressure turbine is compressed from 1·2 kg. per sq. cm. to 2·0-2·5 kg. per sq. cm. by means of a steam jet compressor which is operated by the steam, at 12 kg. per sq. in. pressure, supplied by another back pressure turbine. In this type of plant another steam jet compressor is used to re-compress a certain amount of the 12 kg. per sq. cm. back pressure

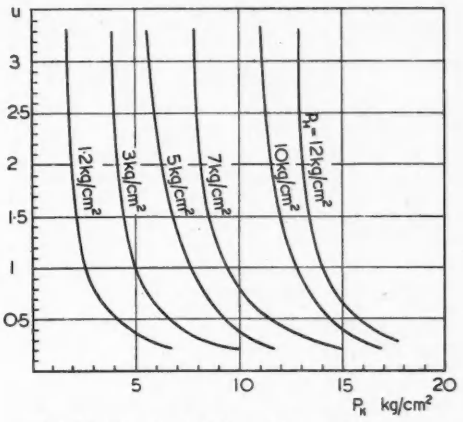

Fig. 2. Injection coefficient characteristics.
(Live steam at p_o = 29 kg/sq. cm. and t_o = 400 deg. C.)

steam to 15 kg. per sq. cm. pressure. This steam jet compressor is operated by live steam of 22 kg. per sq. cm. pressure. Where a turbine with controlled extraction is not available, a steam jet compressor can be employed in conjunction with a turbine without extraction control. In this case, as shown in diagram (f), the steam jet compressor raises the pressure of the uncontrolled

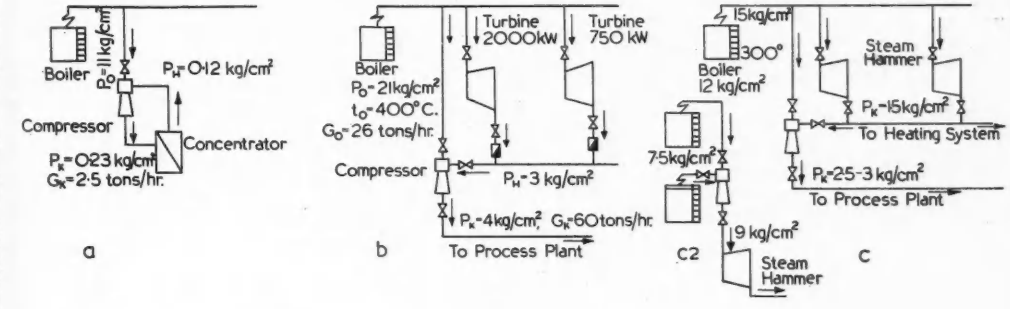

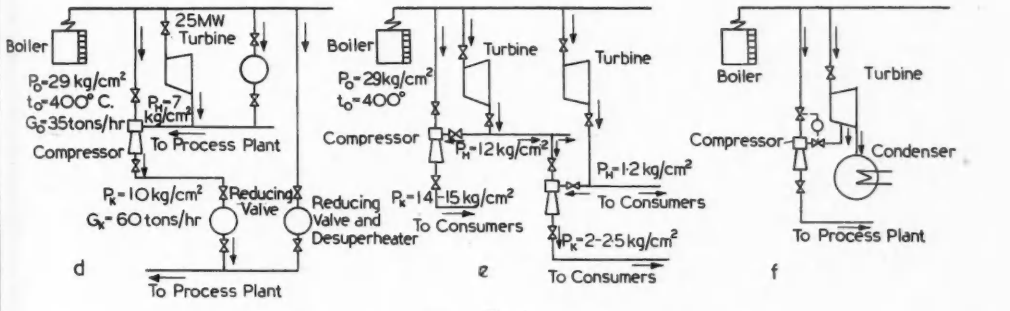

Fig. 1.

(a) Canning factory
(b) Sugar factory
(c) Machine shop
(d) Paper mill
(e) Rayon factory
(f) Turbine plant with uncontrolled extraction rate.

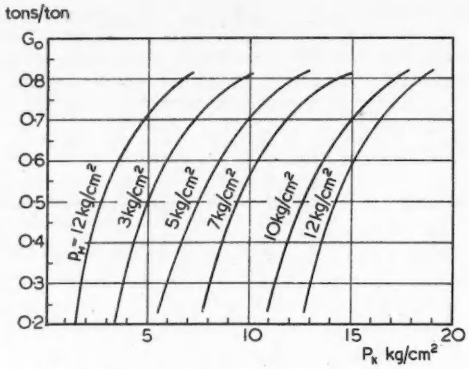

Fig. 3. Live steam consumption per ton of steam compressed.

extraction steam to the pressure called for by process requirements and automatically effects control of this pressure.

If p_o and G_o denote pressure and flow rate respectively of the live steam, p_H and G_H denote the pressure and flow rate respectively of the steam to be compressed, and p_K and G_K denote pressure and flow rate respectively of the compressed steam delivered, then the injection coefficient u is given by

$$u = \frac{G_H}{G_o} = \eta \left(\frac{h_o}{h_1} - 1 \right),$$

and the efficiency of the steam jet compressor will be

$$\eta_o = \frac{h_1 u}{h_o - h_1}$$

The live steam consumption is given by

$$G_o = \frac{G_K}{u + 1}$$

where $G_K = G_o + G_H$, and where h_o is the adiabatic heat drop corresponding to the pressure drop from p_o to p_H in the compressor nozzle, and h_1 is the adiabatic heat increase accompanying the compression of the steam from the pressure p_H to p_K. The efficiency η_o of a well designed steam jet compressor is approximately 22 to 24 per cent. This efficiency range has been used as the basis of the diagram given in Fig. 2 which shows the relationship obtaining between p_K and u for different pressures p_H, the initial steam conditions being $p_o = 29$ kg. per sq. cm. and $t_o = 400$ deg. C. If the injection coefficient u is known, the amount of live steam consumed by the steam jet compressor can be found as

$$G_o = \frac{1}{u + 1}$$

The relationship between G_o and p_K obtaining for different values for p_H is charted in Fig. 3 which is based upon the same initial steam conditions as given above.

These data make it possible to determine the fuel economy that can be obtained with the employment of a steam jet compressor as compared to a pressure reduction installation. Fig. 4 shows the annual fuel saving in tons that can be obtained by substituting a steam jet compressor for a combined pressure reducing and desuperheating installation.

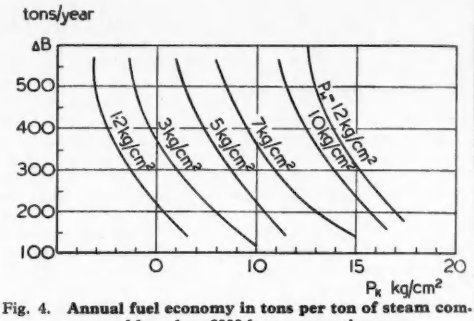

Fig. 4. Annual fuel economy in tons per ton of steam compressed based on 6000 hours operation p.a.
Live steam at 29 kg/sq. cm. and 400 deg. C.

SWITZERLAND

NOVEL THERMOCOMPRESSOR PLANT FOR THE EVAPORATION OF FRUIT JUICES AND MILK

By A. BAUMANN. (From *Brown Boveri Mitteilungen*, Vol. 3, No. 9, September, 1946, pp. 244-246, 6 illustrations.)

IN the evaporation of fruit juices and of milk, heat requirements can be considerably reduced by the employment of the thermocompression system which permits the utilization of the vapour as heating steam. The heat equivalent of the work performed by the compressor in this type of plant is very small and mainly depends upon the temperature difference to be maintained and upon the area of the heating surface, as will be seen from the following data :—

Temperature difference between heating steam and solution, deg. C.	5	10	15	20	25
Heat equiv. of compressor power consumption / Heat of evaporation in %	2·5	5·0	7·5	10·0	12·5

Even where the cost of electric power in terms of calories is two to three times that of coal, the operating cost of the thermocompressor plant amounts to only 15 to 22·5 per cent of that of the coal fired plant without heat recovery, assuming a temperature difference of 15 deg. C. between heating steam and solution. Such a high degree of economy can, however, be attained only if the rise in boiling point of the evaporated medium is small. This is due to the fact that the compressor must produce not only the temperature difference required for the purpose of heat transmission, but it must also overcome the increase in the boiling point of the solution as compared to water. This increase in boiling point is illustrated in Fig. 1 which shows the rise in the boiling point of fruit juice for concentrations up to 42 deg. Baumé ; the graph also shows the amount of water to be evaporated from 1,000 kg. of solution containing 100 kg. of dry matter. A characteristic feature of the process of evaporation is the very rapid increase in the boiling point in the range of higher Bé degrees, this increase being accompanied by a rapid diminution in the amount of water to be evaporated.

The increase in boiling point shown in Fig. 1 is charted in Fig. 2 as function of the amount of water G_w evaporated. If Δt_E is the required temperature difference at the heating surface and Δt_{SP} is the rise in boiling point, then the temperature difference to be produced

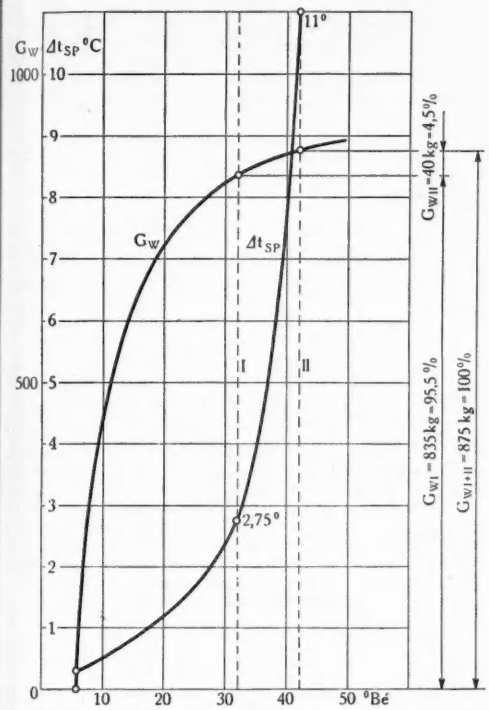

Fig. 1. **Amount of water G_W to be evaporated from 1000 kg. solution (fruit juice) with 100 kg. dry substance and corresponding rise in boiling point *versus* concentration in deg. Baumé.**

by the compressor will be represented by the curve Δt_K and the shaded area below that curve will represent the theoretical power requirements of the compressor. If, however, operation is to be continuous and not in charges, then the load of the compressor will continually correspond to the condition of the final concentration as expressed by the condition Δt_{K_e} in Fig. 2. In this case the work of the compressor as represented by the

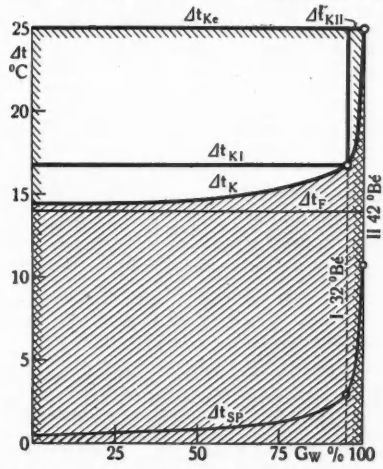

Fig. 2. **Area G_w . Δt_K equivalent to power requirements of compressor for different evaporator circuits.**

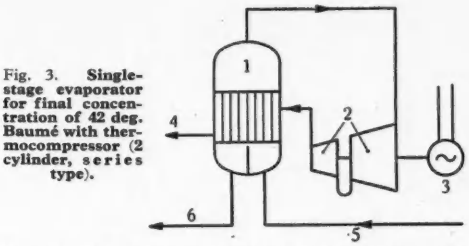

Fig. 3. **Single-stage evaporator for final concentration of 42 deg. Baumé with thermocompressor (2 cylinder, series type).**

area bounded at the top by the horizontal Δt_{K_e} will be approximately 55 per cent larger than that demarcated by the Δt_K curve.

The diagram of a plant of the continuous process type is shown in Fig. 3. But where a concentration of such a high degree is to be attained, it will obviously be preferable to carry out the evaporation process in two successive stages I and II as outlined in Fig. 4. Here

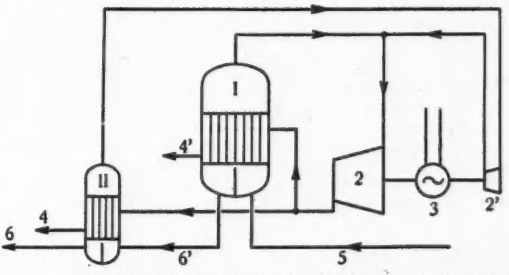

Fig. 4. **Two-stage evaporator for final concentration of 42 deg. Baumé with two thermocompressors and separate vapour removal.**

I = main evaporator
II = final evaporator
2 = main compressor
2′ = pre-compressor
3 = electric drive
4′4 = condensate
5 = solution
6′6 = concentrated liquor of 32/42 deg. Bé

the main evaporator I effects a concentration up to 32 deg. Bé, and the final evaporator II raises the concentration to 42 deg. Bé. In this case 95·5 per cent of the water to be removed will be evaporated in the main evaporator and 4·5 per cent in the final evaporator. In order to preclude the danger of burning the product, a lower working pressure will be adopted for the final evaporator. The respective operating conditions of the two stages will therefore be represented by the lines Δt_{KI} and Δt_{KII} in Fig. 2. The total area demarcated by these two lines is only some 12 per cent larger than the shaded area representing the ideal condition ; vice versa, it is 27 per cent smaller than the area demarcated by the area which corresponds to single-stage evaporation. Two compressors 2 and 2′ (Fig. 4) are employed to remove the vapour from the two stages at the respective pressures and to re-introduce the entire vapour at uniform pressure to the steam chests of the two evaporators. This arrangement secures a thermal saving of 27 per cent as compared to single-stage compression, but it requires the employment of two compressors, or of one compressor with an extraction stage, which is disadvantageous from the aspects of plant design and plant cost.

These drawbacks can easily be overcome by the employment of the system (patent applied for) outlined in Fig. 5, incorporating a single-stage compressor. According to the respective pressures prevailing in the two evaporators, the work of compression is 10 to 15 per cent less than that required in the single-stage system. The essential feature of this arrangement is the ejector 7, shown in Fig. 5, which takes the place of the first stage compressor 2′ (Fig. 4). This ejector utilizes the higher vapour pressure of the main evaporator I to

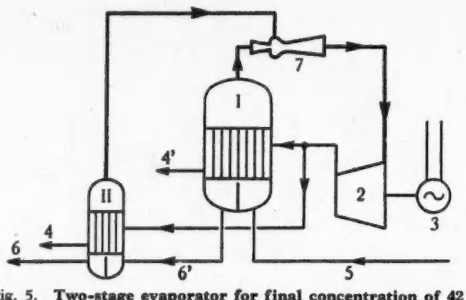

Fig. 5. **Two-stage evaporator for final concentration of 42 deg. Bé according to Brown Boveri system, employing single-cylinder thermocompressor and steam jet ejector-compressor operated by vapour of main evaporator.**

I = main evaporator 32 deg. Bé
II = final evaporator 42 deg. Bé
2 = thermocompressor
3 = electric drive
4'4 = condensate
5 = solution
6'6 = concentrated liquor
7 = jet ejector-compressor

withdraw the vapour from the final evaporator II (which vapour amounts to 5 per cent of the total vapour produced) and to re-compress the total vapour quantity in a diffuser to a pressure closely approximating to that of the main evaporator.

In the case under review conditions are particularly favourable for the employment of the scheme referred to insofar as 95 per cent of the total vapour quantity is available for the compression of only 5 per cent of the latter, so that the action of the thermo-jet approximates to that of a high-efficiency venturi rather than to that of a low-efficiency jet apparatus.

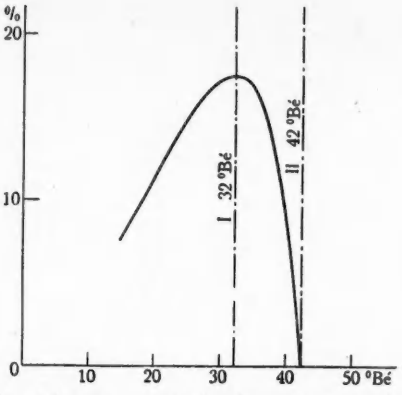

Fig. 6. **Optimum concentration in main evaporator I. (Thermal saving in per cent *versus* deg. Bé).**

As shown in Fig. 6, the limitation of the effect of the main evaporator to a final concentration of 32 deg. Bé affords optimum power economy ; any other distribution of the evaporating effects leads to a diminution in the savings in power consumption that can be derived from this type of plant as compared with the two-compressor system.

BELGIUM

APPROXIMATE CALCULATION FOR SYMMETRICAL SPHERE SPARK-GAPS

By L. MORREN. (From *Bulletin de la Société Belge des Électriciens*, Vol. 62, No. 3, 1946, pp. 91-96, 2 illustrations.)

ALTHOUGH there are several factors, such as temperature and pressure, which affect electrical breakdown it is the electrical field strength which is decisive. This plays a great rôle in the application of spark-gaps which serve either to measure crest voltages or to determine the dielectric strength of solid and liquid materials. Research in the latter field has not gone so far as it has for air because of the greater difficulties encountered. For instance, in the important case of oil, we are far from the regularities which are characteristic for discharges in air and we must still rely on statistical averages.

It is often necessary to compare the results obtained with different instruments. In view of the lack of more accurate information, the electric field only can provide the element of comparison. It should be noted that, according to some theories, the rôle of the electric field is much more decisive in the case of solid or liquid dielectrics than in the case of gases ; (molecular breakdown instead of ionisation by " avalanches ").

It is of importance therefore to calculate, for the usual spark-gaps, the maximum field as a function of the applied voltage. The exact determination of the field is very complicated, but in view of the above considerations an approximate formula should prove sufficient.

MAXIMUM FIELD STRENGTH BETWEEN TWO SPHERES.

The maximum field strength is generally defined by the ratio K which indicates how much larger it is than average ; (the potential difference divided by the distance between the spheres). Ollendorff, in his book : " Potentialfelder der Elektrotechnik " quotes :—

$$K = \frac{V_a \sum_0^\infty n \frac{\sinh(\mu+\lambda n)+\sin \lambda n}{[\sinh(\mu+\lambda n)-\sinh \lambda n]^2} - V_b \sum_0^\infty n \frac{\sinh(\mu+\lambda n)+\sinh \lambda(n+1)}{[\sinh(\mu+\lambda n)-\sin \lambda (n+1)]^2}}{(V_a - V_b)(\sinh \lambda - 2 \sinh \mu)} \quad (1)$$

as the exact solution for K, (V_a and V_b being the potential of the two spheres). λ and μ are given by $\cosh \lambda = (c^2 - a^2 - b^2)/2ab$ and $\sinh \mu = (b/c) \sinh \lambda$; a and b are the radii of the two spheres, c their distance apart. Usually $a = b$ and consequently $\cosh \lambda = (c^2 - 2a^2)/2a^2$ and $\lambda = 2\mu$.

If the distance between the spheres is large when compared with the radii of the spheres, the series (1) converges rapidly. The exact calculations are not then too laborious, but they are also not so interesting. Indeed, the sums in the numerator in equation (1), which are equal for the distance 0 between the spheres, differ more and more as the spheres separate. The equation then shows up the well-known property of spherical systems, that the field depends not only on the geometrical data, but also on the absolute potentials. If they are badly defined, uncertainties are introduced. In practice only two cases need be considered, either one sphere is earthed (potential 0), or symmetrical potentials with respect to zero, which corresponds with the usual test arrangements.

The method proposed here deals with the latter case, i.e. of two equal spheres. This limitation is hardly prejudicial for the following reasons :—

1. We consider mainly dielectric strength tests of insulating materials. Relatively small distances apart are the rule, and in such cases the absolute potentials do not matter ; moreover, the existence of any instruments with unequal spheres is unknown.

2. Apart from the equi-spherical system a flat and a spherical electrode are sometimes used for these tests. K is the same here as in the case of two equal spheres placed at twice the distance apart and subjected to a symmetrical potential.

For small distances equation (1) is, as we have seen, very laborious. A formula by Russel applies to this case but is still too complex for practical purposes. The method proposed below avoids infinite series.

PRINCIPLE OF METHOD.

Just as the field between parallel cylinders is calculated from the field of two parallel linear conductors, we try to solve our problem from the field of two point charges. The equipotential surfaces of two point charges are, however, not spherical and it is impossible therefore to identify one of them with the original sphere.

But we are only interested in the maximum field strength which is produced on the axis at the surface of the spheres where the curvature of the equipotential surfaces is largest.

The field on the surface of a conductor depends on the distribution of the surface charges, which in turn depend on the surrounding field. A satisfactory approximation should therefore be obtainable if the field is only slightly altered in the region concerned.

Though not spherical, the equipotential surfaces of two point charges are of rotary symmetry about the axis they define and as such allow spheres osculating at points on this axis.

If these spheres were made of metal, instead of the real equipotential surfaces, the field in these points would be modified very little. This system now constitutes a spark-gap of two spheres. The problem remains of finding the position of the point charges for which the spheres are osculating with their equipotential surfaces and of working out the field strength and the potential.

FIELD OF TWO POINT CHARGES.

Fig. 1 shows two point charges $\pm q$ at P_1 and P_2 at a distance $2D$. These points define the X-axis about which the field has a rotary symmetry. It is sufficient therefore to consider a plane which contains this axis, in which, half way between P_1 and P_2, (O), we draw a second axis OY perpendicular to OX.

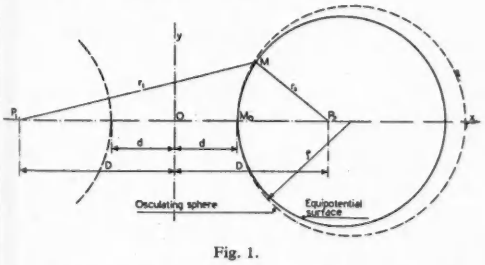

Fig. 1.

The field at a point M with the coordinates x and y, and the distances r_1 and r_2 from P_1 and P_2 respectively, is given by

$$H = \frac{q}{r_1^2} u_1 - \frac{q}{r_2^2} u_2 \quad .. \quad .. \quad (2)$$

u_1 and u_2 being unit vectors in the directions P_1M and P_2M. The potential at this point M is

$$V = q \left(\frac{1}{r_1} - \frac{1}{r_2} \right) \quad .. \quad (3)$$

since the arbitrary constant is 0 in a symmetrical system ($V_0 = 0$).

It can easily be shown that the equipotential surfaces, defined by $1/r_1 - 1/r_2 = \text{const.}$ are surfaces of the 4th degree ; however, we only need the radius of curvature at the apex M_o with the coordinates $x = d$, $y = 0$, of such a surface.

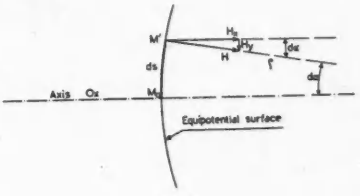

Fig. 2.

M' is a point infinitely close to M_o on the cross section of the surface (Fig. 2), ds the arc, $M'M_o$ and $d\alpha$ the angle between the normals at these two points. The radius of curvature is then given by

$$\rho = \frac{ds}{d\alpha}$$

since the normal at M_o is identical with the axis OX, $d\alpha$ being the angle which the normal makes with the equipotential surface at M', i.e. the direction the field at this point makes with this axis. This angle is given by

$$d\alpha = \left(\frac{-H_y}{H_x} \right)_{M'}$$

Between M and M', $dx = 0$ and $ds = dy$; therefore

$$(H_x)_{M'} = (H_x)_{M_o} + (\partial H_x/\partial y)_{M_o} . ds$$
$$(H_y)_{M'} = (H_y)_{M_o} + (\partial H_y/\partial y)_{M_o} . ds ;$$

For symmetry reasons $\partial H_x/\partial y = 0$, $H_y = 0$, and $H_x = H$; consequently $\rho = (H/(\partial H_y/\partial_y))_{M_o}$

From equation (2) :

$$H_{M_o} = q\,[1/(D+d)^2 + 1/(D-d)^2] = 2q\,.\,[(D^2+d^2)/(D^2-d^2)^2] \quad (4)$$

The same equation gives for the y-component of H in general

$$H_y = (q/r_1^2) . (y/r_1) - (q/r_2^2) . (y/r_2) = qy\,(1/r_1^2 - 1/r_2^2) .$$

Hence

$$-(\partial H_y/\partial y)_{M_o} = q[1/(D+d)^3 - 1/(D-d)^3] = 2q\,.\,d\,(3D^2+d^2)/(D^2-d^2)^3$$

because at M_o $\partial r_1/\partial y$ and $\partial r_2/\partial y$ vanish.

Finally we obtain for ρ

$$\rho = (D^4 - d^4)/d(3D^2 + d^2) \; ; \quad .. \quad (5)$$

and lastly we need the potential in M_o. This follows from (3) as

$$V_{M_o} = q\,.\,[1/(D+d) - 1/(D-d)] = -2q\,.\,d/(D^2-d^2) \quad (6)$$

We consider now a symmetrical spark gap consisting of two equal spheres of radius a at a distance $x = 2d$. We apply the equations (4), (5), and (6), ρ being equal to a, and calculate the value D, which is half the distance of the charges generating the field comparable with the real field. This is the only unknown, because the field and the potential being proportional, the quantity q cancels out in the calculation of K. From equ. (5) we thus obtain

$$D^2 = \tfrac{1}{2} \{ 3ad + \sqrt{[9a^2d^2 + 4d^3\,(a+d)]} \} \quad .. \quad (7)$$

With $m = D^2/d^2$

and $x = 2d$

we obtain

$$m = 3\frac{x}{a} + \sqrt{9\left(\frac{a}{x}\right)^2 + 2\frac{x}{a} + 1} \qquad (8)$$

On the other hand, the total potential difference ΔV between the spheres must be equal to $2V_{M_0}$ (as we have assumed $V_o = 0$), so that for the average field we get $H_m = \Delta V/2d = 2q/(D^2 - d^2)$.

The ratio K is therefore given by

$$K = \frac{H_{M_0}}{H_m} = \frac{D^2 + d^2}{D^2 - d^2} = \frac{m+1}{m-1} \qquad (9)$$

Equations (8) and (9) represent the required solution.

REMARK : A similar procedure could be assumed in the case of two unequal spheres ; but, the simplification due to the symmetry having disappeared, there would be three unknowns instead of one. The resulting equation would be of the sixth degree.

NUMERICAL VALUES.

Given below in Table I are the values K_f derived from equations (8) and (9), and K_e derived from the exact equation (1) together with the relative error ϵ_f.

TABLE I.

Relative Distance x/a	Coefficient K		Error
	K_f (formula)	K_e (exact)	ϵ_f in per cent
0·12	1·0405	1·0403	+ 0·02
0·4	1·1390	1·1371	+ 0·17
0·8	1·2881	1·2827	+ 0·42
1	1·3660	1·3590	+ 0·51
1·6	1·6105	1·6006	+ 0·62
2	1·7808	1·7703	+ 0·59
3	2·2247	2·2148	+ 0·45
5	3·1583	3·1513	+ 0·22
12	6·5760	6·5738	+ 0·03

The error, being initially zero, passes through a maximum and then tends again towards zero for large distances. The limit of both expressions is

$$K = \tfrac{1}{2}(x/a + 1)$$

This can be justified intuitively as follows :

If the distance between the spheres is small compared with the radius of curvature of the equipotential surfaces, the osculating sphere will have almost the same shape as the electrode for a comparatively large area about the axis. The field is therefore practically correct.

For great distances the explanation is that equipotential surfaces very close to the point charges are very nearly spherical and may therefore be superimposed on the real spheres with a good approximation.

The maximum error is close to the relative distance $x/a = 1{\cdot}6$ and reaches a value of slightly more than $\frac{1}{2}$ per cent.

APPLICATIONS.

(A) Comparison of Different Specifications for Oils.

The different national standard specifications,—the Belgian (C.E.B., rapport no. 13), the French (U.S.E. 136), the British (B.S.S. 148), and the German (V.D.E. 0370),—demand certain strength tests for oils by means of bi-spherical spark gaps, different in each case. Furthermore, while the German specifications require a minimum break-down field, the three others demand a minimum break-down voltage under defined test conditions.

These different requirements will now be compared by the determination in each case of the maximum field. By definition this is

$$K\frac{\Delta V}{x} \text{ or } M\Delta V \text{ with } M = \frac{K}{x}$$

The German V.D.E specification anticipates variations in x ; yet, the German instruments carry a graduation showing directly the maximum field strength for a distance of 3 mm. Hence, if this distance is to be reduced to x', the reading must be multiplied by M'/M, a value which is thus equally useful to determine.

Table II shows the characteristics of different spark-gaps and the values of the corresponding coefficients.

TABLE II.

Specification	Radius of spheres mm.	Distance absolute mm.	Distance relative mm.	K	M cm^{-1}	$\frac{M'}{M}$
C.E.B.	5	2	0·4	1·14	5·70	—
U.S.E.	6·25	5	0·8	1·29	2·58	—
B.S.S.	6·5	4	0·62	1·22	3·05	—
V.D.E.	25	3	0·12	1·04	3·47	1
V.D.E.	25	2	0·08	1·027	5·135	1·48
V.D.E.	25	1	0·04	1·013	10·13	2·92

Based on this, Table III gives the comparison between the dielectric properties required by the different specifications.

TABLE III.

Specification	Oil	Minimum Voltage	Maximum field $H_{max} = M\Delta V$ V/cm.
C.E.B.	new	18,000	102,500
C.E.B.	new, dehydrated	25,000	142,500
U.S.E.	new	40,000	103,000
B.S.S.	new	30,000	91,500
V.D.E.	in service	—	80,000
V.D.E.	ditto, dehydrated or prepared for filling	—	125,000

The Swiss specifications have not the break-down field strength as the criterion for oil ; they recommend an endurance test of 30 minutes with an instrument with two similar spheres at a distance required under the French specifications. This test is made with new oils either under a tension of 30 kV or under a maximum field strength of 77,500 V/cm.

The American specifications (A.S.T.M. D 117-36) are not directly comparable with the European ones, because their electrodes are flat sharp edged disks of one inch diameter placed in parallel and spaced 1 in. apart. For new oils they demand a minimum voltage of 25,000 V, i.e. an average field strength of 98,500 V/cm.

For new oils the different specifications are therefore comparable within approximately 10 per cent.

B. Tests for Insulating Plates.

The specifications of the Comité Electrotechnique Belge for the dielectric strength tests of insulating plates require that the tension be applied between a plane electrode on one side of the plate and a spherical segment of 25 mm. radius, placed in a cavity of equal shape, on the other side. The depth of the cavity is such, that the smallest thickness of material left is approximately 3 mm. A tolerance of $\pm$ 0·5 mm. is allowed for this thickness. It has therefore to be measured in every case. The conversion from break-down voltage to the maximum break-down field strength again furnishes the possibility of comparing results. We again therefore need a table of coefficients M as a function of the thickness. This is given below (Table IV), as calculated on the basis of the foregoing considerations.

TABLE IV.

Minimum Thickness mm	Coefficient M cm^{-1}
2·5	4·27
2·6	4·12
2·7	3·98
2·8	3·84
2·9	3·72
3·0	3·61
3·1	3·50
3·2	3·40
3·3	3·31
3·4	3·22
3·5	3·13

THE PANT-O-JECTOR METHOD OF GAUGING.

By E. C. POLIDOR, Chief Engineer, Engineers Specialities Division, Buffalo—Cleveland—Rochester.

WITH the coming of jet propulsion, many new problems have developed bringing many new devices and techniques to industry. A fast and accurate method of inspecting blade and bucket profiles has been a problem of major importance—for without full knowledge of this important " corner " of the complete development, progress would be retarded.

All inspection problems involve basic considerations which are as follows :—

1. Accuracy of the gauging device
2. Ease of operation
3. Maximum rate of inspection without sacrifice of accuracy
4. Elimination of " human element " or personal judgement
5. Ability to ensure " repeat " answers
6. Flexibility
7. Wear consideration.

The Pant-O-Jector embodies the highest quality of engineering skill and workmanship. Features have been incorporated to check a multiplicity of problems which have been presented by many different concerns actively engaged in the jet propulsion field.

The principle of the Pant-O-Jector is simple. Since it is not possible to gauge the actual surface of the blades or vanes other than by use of templates, formed to exact specifications, or by measuring co-ordinate points from given datum lines, the resulting conclusion is a pantograph.

A pantograph works on the principle of a parallelogram which ensures a duplicate motion from follower to scribing point. There are many forms of pantographs, we use the simplest form—the " X " and " Y " motion. We also felt that there were many advantages to " tracing the path " of the scribing end of a pantograph on a projection instrument at a known magnification. Pantograph on a projector—or " Pant-O-Jector "*—is the logical name.

All the basic units we have developed for checking blades or vanes follow the same principle—" X " and " Y " displacement—as nearly perfect motion in the horizontal and vertical planes as is possible to build. It must be as nearly perfect as possible ; for without this accuracy the desired results cannot be attained. These units are built so that as the base travels in the horizontal plane another moving part, the " sleeve," can move in the vertical plane guided by an upright " post," fastened to the base which moves in the horizontal plane. In other words—you can go " up " and " down " and the " across " motions are exactly 90 degrees apart, and these units are made to stay that way because both motions are assembled using " pre-loaded " ball bearings and made so that if wear should occur, it can be corrected very easily.

Obviously, the " up " and " down " motion and the " across " motion itself, cannot gauge a blade. However, by placing a projecting arm on the " sleeve " and letting the end of the arm contact the blade surface, then as it moves " across " the blade, the end of the arm will guide the " up " and " down." Then we placed another projection on the sleeve which has the same shape as the end of the first arm and it is the shadow of this arm that is projected on the screen. Whatever movement is made by the follower is also made by the projected end, and this is positive because the " X " and " Y " motion ensures this result.

The follower that follows the blade profile should be a radius and the shadow projected on the screen should be identical in shape and size. We use a roller and a hole, or " eye," because whatever path the roller followed, the " X " and " Y " motion of the Pant-O-Jector guaranteed perfect transmission of motion to the hole, or eye, and, therefore, by following the path of the eye on the screen an accurate transcription of the blade profile is definitely seen.

One of the main features of the Pant-O-Jector unit is that it can be used on standard comparators having a fourteen-inch diameter or larger screen. Chordal lengths of average blades are from one inch to two and one-half inches. At ten magnifications this would mean that the section lengths on the screen would be from ten to twenty-five inches long on a fourteen-inch screen, but it is possible to split this line into two parts. By positioning it properly it would represent one complete profile. In order to accomplish this, the unit has two, and in some cases three, eyes spaced according to specifications, usually exactly one inch from centre to centre. When proper co-ordination between chart-gauge and fixture is obtained, one hole or " ball " may be seen on the screen as the roller starts to travel across the blade. However, as this " ball " approaches the edge of the chart-gauge, another " ball " appears on the screen at the opposite edge of the chart-gauge ; and it will follow a continuation of the same profile the original " ball " was following.

There are many variations of the Pant-O-Jector, all however, on the same identically sound principle.

Fig. 1 represents a model which can be used for checking one side of the blade at a time. The roller and the " eye " are both fastened to the vertical " sleeve " and through the " X " and " Y " motion the true path of the blade is described. It is designed to fit all standard comparators having fourteen inch or larger diameter screen. Although only two " eyes " are shown, replaceable brackets of one, two, three or more eyes can be used.

Fig. 2 shows the same style Pant-O-Jector with the double arms which eliminate the necessity of revolving the blade 180 degrees. It does not check both sides at one time, but is made to check one side when " down " pressure of the " sleeve " is applied and opposite side of the blade when " up " pressure of the " sleeve " is applied. In this case, a double " eye " bracket is used and is required to have the same centre to centre spacing as the rollers. If this relationship were not maintained, then the true sectional outline of the blade would not be checked, since spacing error would have the effect of showing the blade as being thick or thin. This unit can also be used on all standard comparators.

Fig. 3 is a unit for checking both sides simultaneously. The principle is the same. A cross-beam moves up and down and superimposed on this cross-beam are two " sleeves " which move independently on ball bearings.

* Patent pending.

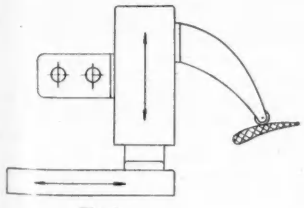

Fig. 1

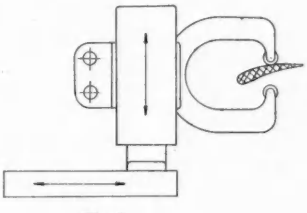

Fig. 2

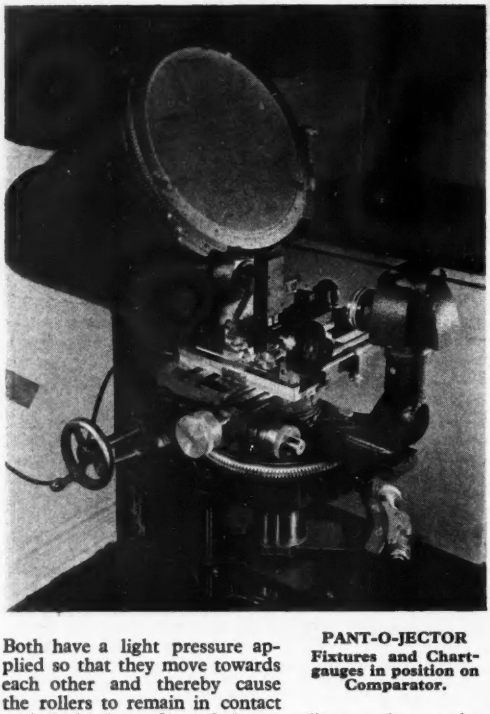

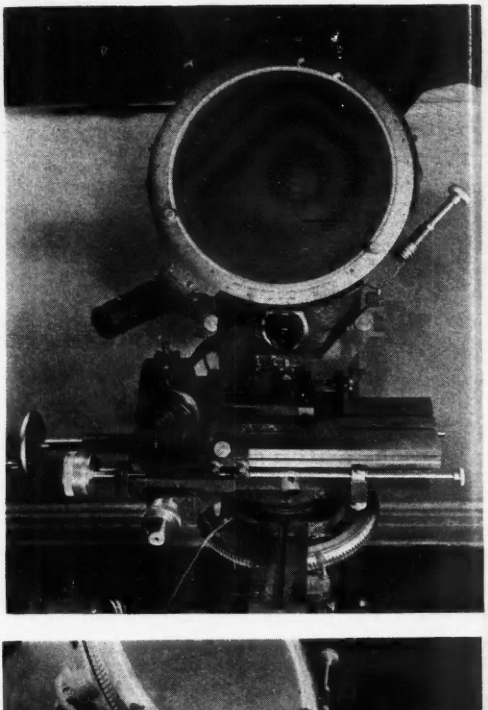

PANT-O-JECTOR
Fixtures and Chart-gauges in position on Comparator.

Both have a light pressure applied so that they move towards each other and thereby cause the rollers to remain in contact with the blade profile. Only one roller at a time can be applied if desired. A special comparator has been used for this unit, although with some modifications it can be made to fit standard comparators.

Fig. 4 is another variation of the same principle. This unit can be made to fit all comparators and is particularly suited for checking dies.

Pre-loaded ball bearings guide all the movements and the assembly is designed so that they remain in this desirable condition with only a minimum of adjustment necessary.

When using the Pant-O-Jector, the chart-gauge has an outline exactly to drawing specifications. We can furnish 1 to 1 prints on metal, and by machining and filing to the contour line, an accurate template can be made. This same metal reproduction can be done at 10× and 20× and higher magnifications, so that they can be used in connection with profile grinders. Metal charts can be made to be used in connection with direct projection, and, of course, transparency chart-gauges in any quantity can be made from the same original accurate master scribing. Chart-gauges made to be used in conjunction with the Pant-O-Jector, are easy to check. Simply lay them over a universal grid chart and

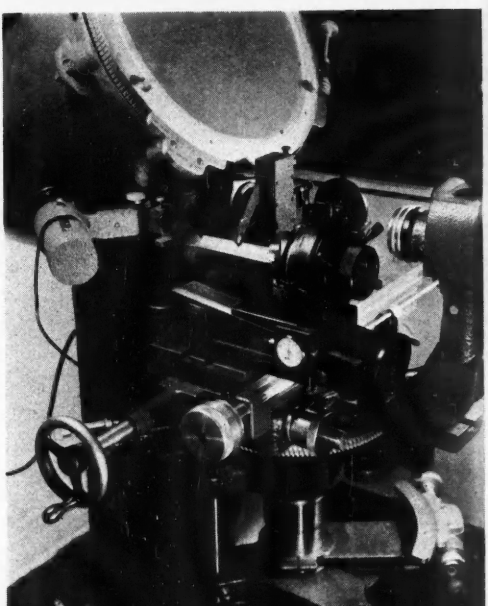

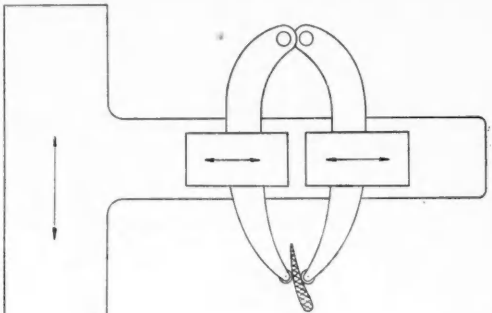

Fig. 3

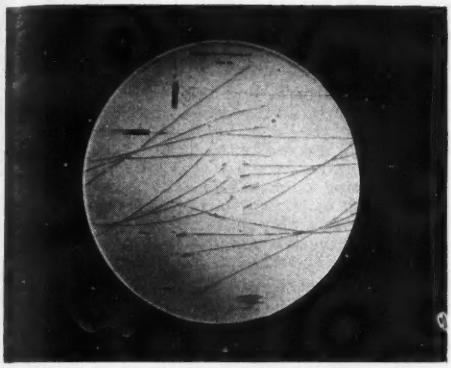

Chart-gauge for inspection of a 1·500 in. width 4 section blade.

The chart-gauge shows two contour lines for each of the four sections—one for top surfaces and one for bottom surfaces. Due to the width of the blade (1·500 in.), the full contour of any section would extend beyond the limits of the screen. For this reason the contours are broken into two overlapping sections co-ordinated to the centre-line distance of the two viewing " eyes " of the Pant-O-Jector. The upper and lower contours are further separated to eliminate any confusion from superimposed lines.

The small cross-marks on each contour indicate the co-ordinate points which determine its shape. The length of each of these marks indicates the permissible tolerance at each point. In the upper left-hand corner the two set master lines appear flanked by scales of parallel lines. These scales represent the allowable twist of the blade and are read with the Panto-O-Jector in setting position.

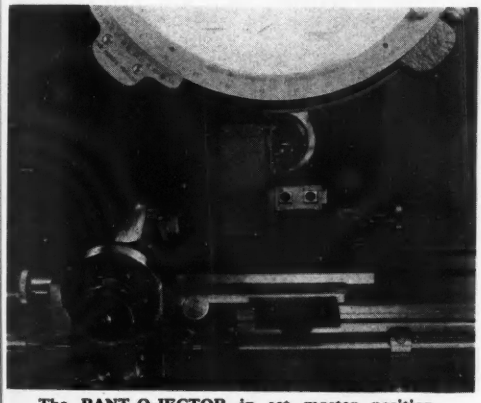

The PANT-O-JECTOR in set master position.

Before proceeding with inspection, the Pant-O-Jector is brought into alignment with the chart-gauge by placing the traverse arm in this, the setting, position. The image of the " eye " on the screen should then align to the two set master lines.

count the squares to as many intersection points as required.

In the original designs of the Pant-O-Jector we planned the use of a " fixed " hole or " eye " as a follower. The " eye " can be in any convenient position and the only requirement is, that it be fastened to the same moving " sleeve " to which the tracer end is fastened. In further consideration of the problem, we felt that if the " eye " did not follow the prescribed line, it would be desirable to shift the " eye " " X " and " Y," and thereby find the correct position so that the " eye " would follow the line. This would mean that the form of that particular section is correct, but that its *location* is incorrect. This is a very common error: since the blade profiles are uniform in shape, but due to excessive heat required in the forming operation, there is often a distortion caused by the cooling.

The " moving eye " feature has been used very

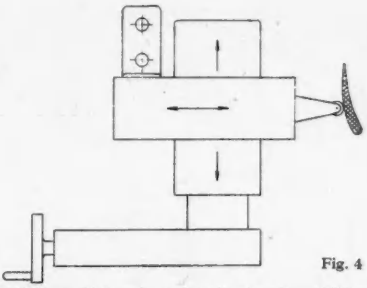

Fig. 4

successfully and its operation is simple. This is illustrated in Fig. 5. By turning A the " eye " moves laterally and B moves the " eye " vertically, i.e. an " X " and " Y " motion superimposed on the " X " and " Y " movement of the Pant-O-Jector is carried out. When starting to check a blade, the roller is prepositioned in a " set " location of the fixture. This " set " position is located properly with the work holding fixture and is generally associated with the theoretical centre of gravity of the blade. When in this " set " position, the " eye " is moved into the " set " lines on the chart-gauge as shown in Fig. 6. The " set " position shown on the chart-gauge is also located with the centre of gravity of the blade outline shown on the chart-gauge. If the blade is correct, the " eye " will follow the shape on the chart-gauge. However, if the " eye " scribes a path shown by the dotted line C, for example, it appears that the shape is correct, but the location of the section does not meet specifications. In order to determine this, turn knob A which moves the " eye " to the left, and knob B which elevates the " eye," until the " eye " follows a prescribed path. We find that the shape of that particular section is correct ; the centre of gravity, however, is not located properly. To determine how much " off

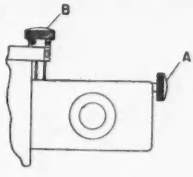

Fig. 5

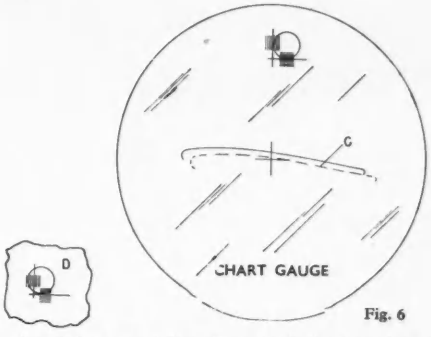

Fig. 6

location " the centre of gravity actually is, drop the roller back into the original " set " position of the fixture ; it is noted that the " eye " has been moved as shown at D, and it can be determined by the scale, that the centre of gravity has been displaced vertically ·002 in. and horizontally ·006 in.

There are many other devices which aid in determining exactly what is wrong with a blade profile which

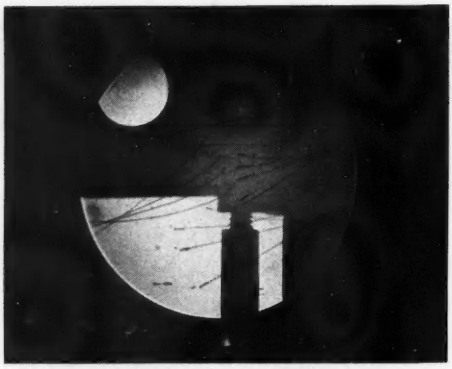

Eye aligned to set master.
With the shadow in this position, the chart-gauge is accurately aligned and co-ordinated with the Pant-O-Jector and blade holding fixture.

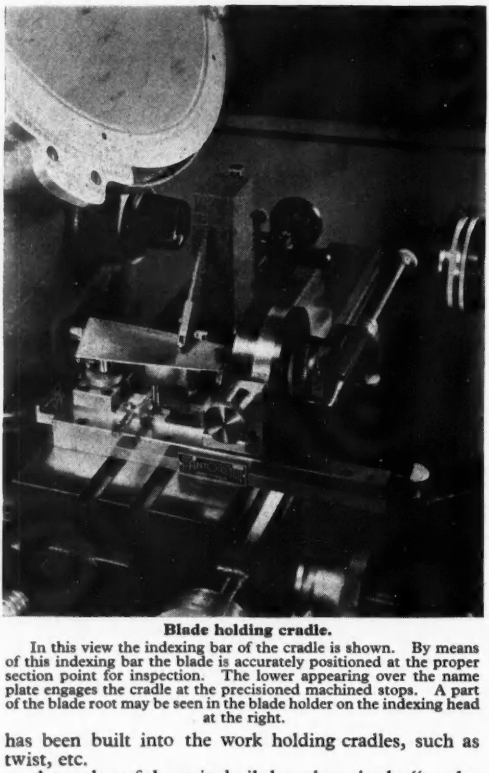

Blade holding cradle.
In this view the indexing bar of the cradle is shown. By means of this indexing bar the blade is accurately positioned at the proper section point for inspection. The lower appearing over the name plate engages the cradle at the precisioned machined stops. A part of the blade root may be seen in the blade holder on the indexing head at the right.

has been built into the work holding cradles, such as twist, etc.

A number of the units built have been in the " analytical " class. There is a logical reason for this. Up until the Pant-O-Jector was used, there was little or no chance to " study " a blade. Template gauges were the only devices used, and these are impractical from a standpoint of study. It is obvious that in order to improve a product it is essential to know exactly what your product is, and make corrections from there on. " Analytical " devices are therefore essential.

The use of the Pant-O-Jector, however, is not confined to the analytical class. It must be kept in mind that one of the principal reasons for using an analytical fixture is to study the blades and determine what variation can be expected due to forging or casting operations. Permissible variation in shape and position (centre of gravity) can be determined at specific points along the contour.

From this, a chart-gauge can be developed, showing the tolerance lines. The blade is acceptable, providing that the edge of the " ball " of light follows between the minimum and maximum tolerance lines. In actual practice, inspection by this method is very satisfactory. It leaves nothing to the judgement of the operators.

The fixture used for production inspection of finished blades is different and faster than the analytical type fixture. Indexing the blade from section to section is done rapidly and positively. Instead of a hand wheel and screw arrangement for operating the Pant-O-Jector, which is desirable when a study is to be made, a lever is used on the production unit. Production inspection units for rapid inspection used for checking one side of the blade at a time, incorporate a lever arrangement for rapid and positive 180 degree rotary index. Units to check both sides of the blade simultaneously are also supplied.

There is still another type of production inspection unit which has been designed and built. This unit is a logical answer to the problem of inspecting, *before* any machining work is done on the " root " or " dovetail " as it is often called. As explained by the various manufacturers, the blade profile, because of compara-

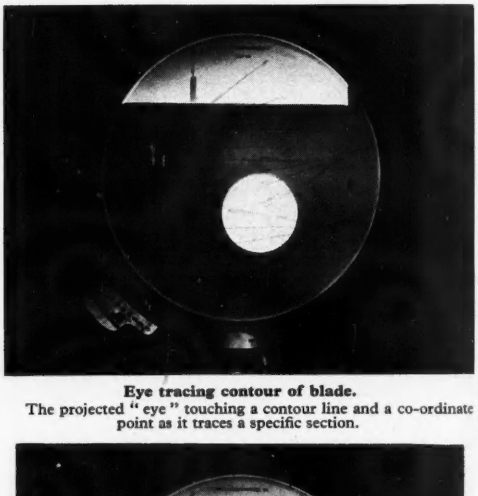

Eye tracing contour of blade.
The projected " eye " touching a contour line and a co-ordinate point as it traces a specific section.

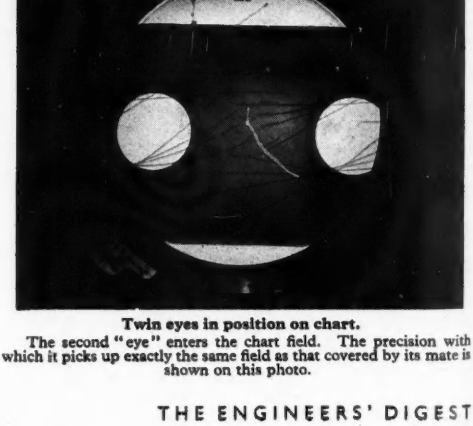

Twin eyes in position on chart.
The second " eye " enters the chart field. The precision with which it picks up exactly the same field as that covered by its mate is shown on this photo.

tively uniform cross-section, may vary slightly in form. Because of greater " mass " of material, the relationship of the root to the blade and the variations in the root itself are quite pronounced. The problem is to locate a working surface with relation to the blade profile, and then in subsequent operations, finish the root from this working surface. By this method only a minimum of operations need be done to produce an acceptable blade. A " forged " or " cast " blade has more than sufficient stock left on the root to take care of all variations in relative location of the blade. A blade holding fixture is designed so that the root is gripped in locking jaws of the work holding cradle and, while held in this manner, the entire blade can be moved into any position. This is done in a " ball-socket " type holding fixture which permits angular positioning. It is also possible to obtain a rotary motion, a vertical, and a horizontal motion.

The Pant-O-Jector unit checks both sides of the blade simultaneously. Having the chart sections positioned properly, the problem is, therefore, to move the blade into the correct profile, without consideration of the root location. By means of the four adjustments, angular, rotary, vertical and horizontal, this can be done quickly. When the blade profile is thus in the correct position, a built-in drill in the fixture is used to drill a small centre in each end of the blade or two centres at one end and one at the opposite end. The centre drills are prepositioned in relation to the chart-gauge, and these do not change location while the blade is being moved into the prescribed chart sectional layouts. The centre drills have, therefore, established the centre of gravity of the blade, and when it is removed from the jaws all subsequent operations are done with relation to these centres—the centre of gravity of the blade.

RUSSIA

RESISTANCE OF CONTACT BETWEEN METALS, AND BETWEEN METALS AND CARBON MATERIALS.

By Yu. V. Baimakoff. (From 3rd Technical-Scientific Conference of the Kalinin Polytechnic Institute, Leningrad, September, 1944, p. 50.)

Electro-chemical and electro-metallurgical plants employ a great variety of contacts under widely varying conditions. The electrical resistance of these contacts has a considerable influence on the efficiency of such plant. The author has found, for instance, that the drop in voltage at the contacts used in baths for aluminium electrolysis amounts to between 5 and 20 per cent of the total voltage available.

Results are given of experiments on the effect on contact resistance of pressure and of a temperature high enough to cause oxidation of the contact faces. The effect of pressure was found to be considerable and to be the greater the more plastic the metal. For example, a rise in pressure from 30 kg./sq. cm. to 630 kg./sq. cm. reduced the resistance between two metal surfaces (consisting of copper, aluminium, brass or cast iron) to between $^1/_9$ and $^1/_{15}$. Table I shows data which may help to select contact materials and to calculate their resistance. Figures are given for contact pressures of 150 and 600 kg./sq. cm. The latter pressure was also applied when bedding-in the contacts.

The influence of heat on contact resistance varies; in some cases, resistance is increased owing to oxygen diffusion into the area truly in contact, in others the resistance is not changed, or is even reduced when the two metals are in complete contact.

While Table I deals with resistance contacts between two metals, Table II indicates contact resistance between metals and carbon materials. The variation of the resistance between metal and carbon, when subject to heating, is caused by the penetration of oxygen through the pores of the graphite or carbon contact and influenced by the rate of growth and by the conductivity of the oxide layer.

Pressing a metal core into carbon, followed by baking, results in a resistance between 0·55 and 3·5 ohm./sq. cm., depending upon the quality of the carbon and the baking temperature. In this case, heating causes an increase in resistance owing to oxidation of the metal. Such contacts may be used at temperatures as high as 800 deg. C. when fully shielded from oxygen.

Contacts produced by casting non-shrinking cast iron into carbon are not very reliable. The cast iron used should contain between 4·8 and 5·5 per cent Si; a contact resistance of 2-3 ohm./sq. cm. has been measured, but it varies a great deal. Another cast iron may have a resistance of up to 10 ohm./sq. cm.

Carefully scraped contact surfaces, under pressures between 150 and 600 kg./sq. cm., do not change their resistance even under very severe operating conditions. The best among the carbon-metal contacts are those consisting of carbon, and a metal pressed into carbon, followed by baking.

Table I.

Contact materials	Pressure, kg./sq. cm. 150	Pressure, kg./sq. cm. 600	Effect of heating to 300 deg. C. for 120 hr.
	Resistance, ohm/sq. cm. × 1/1000		
Copper-Copper	0·13	0·03	No change (800 deg. C.)
Aluminium-Aluminium	7·5	1·8	Increase 3 times.
Brass-Brass	1·5	0·6	Drop to ½.
Cast Iron-Cast Iron	30	12	Increase 4 times.
Steel-Steel	8·5	2·7	Drop to ½.
Tinned Copper-Tinned Copper	0·34	0·08	No change.
Copper-Aluminium	1·3	0·40	No change.
Copper-Cast Iron	6	4·4	Increase 5 times.
Copper-Steel	1·5	0·39	Drop to 1/5.
Brass-Aluminium	4·5	0·76	Increase 4 times.
Brass-Cast Iron	8·9	3·2	Increase 5 times.
Aluminium-Cast Iron	11	0·85	Increase 20 times.
Aluminium-Steel	6	1	Increase 40 times.
Steel cast into Cast Iron	Between 19 and 49.		Depends upon casting temperature

Table II.

Contact materials	Pressure, kg./sq. cm. 30	Pressure, kg./sq. cm. 150	Effect of heating to 300 deg. C. for 120 hr.
	Resistance, ohm/sq. cm.		
Copper-Carbon	0·085	0·050	Increased 10 times.
Copper-Graphite	0·040	0·017	Increased to infinity.
Brass-Carbon	0·50	0·15	Reduced to 1/5.
Aluminium-Carbon	0·36	0·09	
Aluminium-Graphite	0·09	0·050	Increased to infinity.
Cast Iron-Carbon	0·50	0·14	Increased 5 times.
Cast Iron-Graphite	0·12	0·052	Increased 12 times.
Steel-Carbon	0·30	0·21	Reduced to 1/5.
Steel-Graphite	0·16	0·050	Increased 7 times.

RUSSIA

HEAT DISTRIBUTION AROUND THE WELDING ARC

By N. N. RYKALIN. (From *Avtogennoe Delo*, No. 2, 1946, pp. 6-11, 11 illustrations.)

THE theoretical study of heat distribution around the electric welding arc is important, but not easy considering that apart from the geometrical variety of articles to be welded the arc power may vary from 0·3 to 150 KW., and the speed from 0 to 650 ft./hour, that the temperatures involved can reach 5000-6000 deg. C. (i.e. above boiling point of metal) and that the concentration of heat flow amounts to over 20,000 calories per sq. in. per sec. at the " heat spot " of the arc.

The best approach to the problem is to deal with three " ideal cases " from which other and more practical examples may be derived. These cases are :

(*a*) (Figs. 1a and 2a) A point source of heat *O* travelling over a solid body.

(*b*) (Figs. 1b and 2b) A linear source of heat *O* travelling over a thin plate of thickness δ.

(*c*) (Figs. 1c and 2c) A laminar source of heat travelling along a rod of small cross-section *F*.

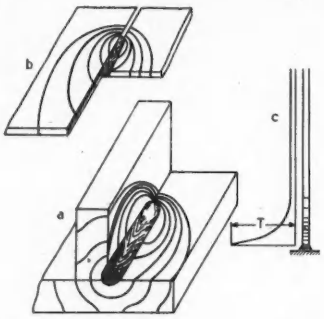

Fig. 1. **Temperature zones round an arc : three, two and one dimensional.**

In all three cases it is assumed that the bodies affected are of infinite extent, i.e. in case *a* the body is of a semi-infinite size, in *b* the plate is of infinite area and in *c* the rod is infinitely long.

Heat will spread along the body according to the differential equation (Fourier) :—

$$\frac{\partial T}{\partial t} = a \nabla^2 T \quad \ldots \quad \ldots \quad \ldots \quad (1)$$

while the surfaces of the heated bodies may either be assumed to be a complete barrier to the passage of heat or to radiate it according to Newton's law :—

$$\frac{\partial T}{\partial n} + \alpha T = 0 \quad \ldots \quad \ldots \quad (2)$$

The phenomena under investigation take place under such wide a range of temperatures that the various thermal coefficients are far from constant as shown in Fig. 3 for mild steel.

In addition, chemical changes take place which involve thermal reactions.

It is usual, however, to take constant average values for λ, c, a, and α, whereupon equations (1) and (2) become linear and yield workable solutions.

The study of the effects of a moving source of heat is best carried out as proposed by Kelvin and Raleigh, i.e. by regarding them as due to a series of instantaneous point sources, the individual effects of which are superimposed one upon another.

Considerable simplification is possible by referring the results to a system of coordinates which is assumed to be moving together with the source of heat and by an extensive use of non-dimensional criteria (parameters). One particularly important solution is that for " settled conditions," i.e. for temperature distribution with respect to the arc during an infinitely long run. This, of course, is one of the cases where a moving system of coordinates must be used.

If a welding run is made on an infinitely thick body, then the temperature distribution, for settled conditions, is expressed by the function :—

$$T(R, x) = \frac{2}{2\pi\, 2R} \exp\left(-\frac{vx}{2a} - \frac{vR}{2a}\right) \quad (3)$$

where q = quantity of heat in calories = 0·24 × Amps × Volts × η_u and where η_u = coefficient of heat transmission of the arc to the welded body. The corresponding temperature curves are shown in Fig. 4 (calculated for mild steel with q = 1000 Cal./sec. and v = 0·1 cm./sec.).

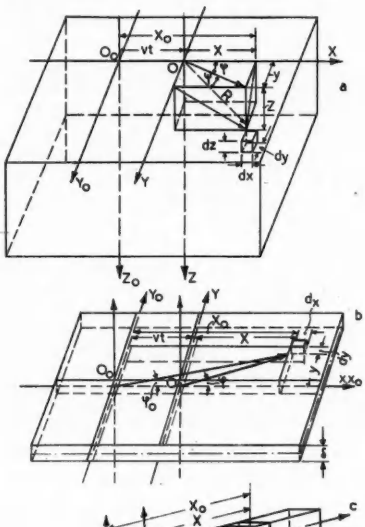

Fig. 2.

For two thin sheets butt-welded together the equation is :—

$$T(r, x) = \frac{q}{2\pi\, \lambda\delta} \exp\left(-\frac{vx}{2a}\right) K_o\left(\phi \frac{vr}{2a}\right) \quad (4)$$

where $$\phi^2 = 1 + \frac{8\,\lambda\alpha}{\delta(vc\gamma)^2}$$

and γ = density of metal.

The result is shown in Fig. 5 for steel sheet 1 cm. thick, q = 1000 Cal./sec., v = 0·1 cm./sec. and α = 0·0014 Cal./cm.²/sec./deg. C.

The flow of heat through the body comprises three phases :— (*a*) heating up, during which the temperature rises relative to the moving coordinates. (*b*) settled

conditions as described above and (*c*) levelling out of temperatures after welding is finished.

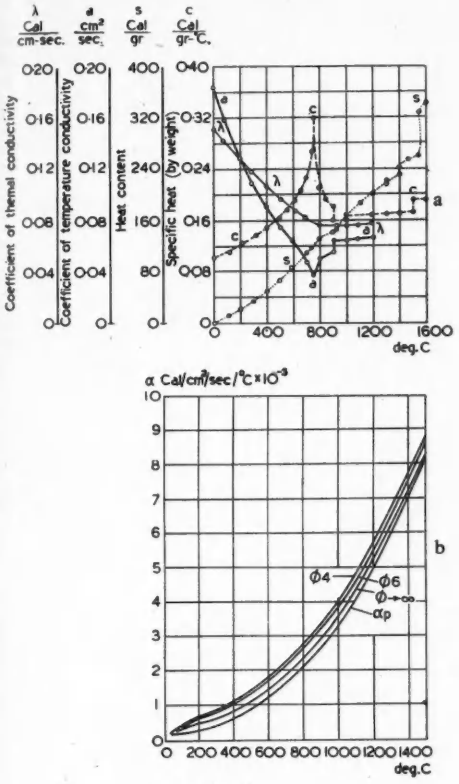

Fig. 3.

(a) "Constants" λ, a, s, c.

(b) **Coefficient of heat loss from surface (α) for vertical plate (αp) and rods of various diameters (in mm.)**

EFFECT OF ARC MOVEMENT.

Near the arc, phase (*b*) is attained very quickly and therefore only phase (*a*) has to be considered at points well away from the arc. The quicker the movement of the arc, the quicker settled conditions will be attained at a given distance from it. In a typical example, points 2 cm. away from the arc reached settled conditions within 60, 25, and 9 secs. respectively with the speed of the arc varying from 0·1 to 0·2 and 0·3 cm./sec.

The temperature curves which, with stationary arc, are a series of concentric circles become elongated behind the moving arc and "bunch" together in front of it. The greater the speed, the greater the elongation as well as the bunching, as shown in Fig. 6 (for mild steel plates 1 cm. thick and q = 1000 Cal./sec.). In the case of extremely rapid movements and strong arcs, the temperature equations tend to a limiting value:—

(*a*) for a welding run on thick metal

$$T(t, y_0, z_0)\Big|_{v \to \infty} = \frac{q}{2\pi\lambda vt} \exp\left(-\frac{y_0^2 + z_0^2}{4at}\right) \quad (5)$$

and (*b*) for sheets

$$T(t, y_0)\Big|_{v \to \infty} = \frac{q}{v\delta\sqrt{4\pi 2c\gamma t}} \exp\left(-\frac{y_0^2}{4at} - \frac{2\alpha t}{c\gamma\delta}\right) \quad (6)$$

where $t = -\frac{x}{v}$ = time which has elapsed since the arc passed the point under consideration.

These equations, being related to the fixed coordinates x_0 y_0 z_0 are often more convenient to handle than equations (3) and (4), and, in particular, they are perfectly applicable to the analysis of conditions in a long narrow zone behind the arc for the higher speeds and arc intensities which are frequently used. Thus, in the unshaded part of the work shown in Fig. 7 (q = 5000 Cal./sec., v = 1 cm./sec.) the temperature error introduced by using expression (5) instead of (3) is less than 1 per cent.

The maximum temperature at a distance r_0 (or y_0) from the travel of the arc is, according to Rykalin (see ref. 10), for a thick body

$$T_m(r_0) = \frac{1}{R} \times \frac{q}{\frac{\pi}{2} r_0^2 vc\gamma} \quad (7)$$

and for a sheet

$$T_m(y_0) = \sqrt{\frac{2}{\pi e}} \times \frac{q}{2y_0 vc\gamma\delta}\left(1 \frac{\alpha y_0^2}{\lambda\delta}\right) \quad (8)$$

i.e. the temperature varies inversely as r_0^2 for the thick body and approximately as $\frac{1}{y_0}$ for the sheet.

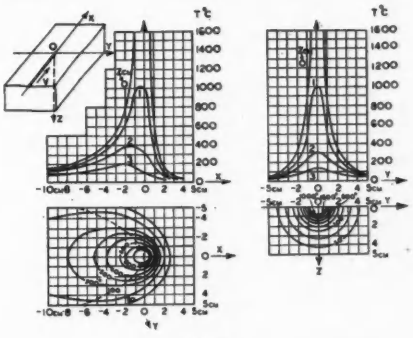

Fig. 4.

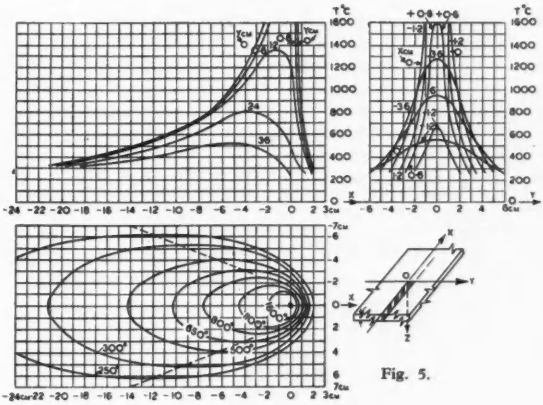

Fig. 5.

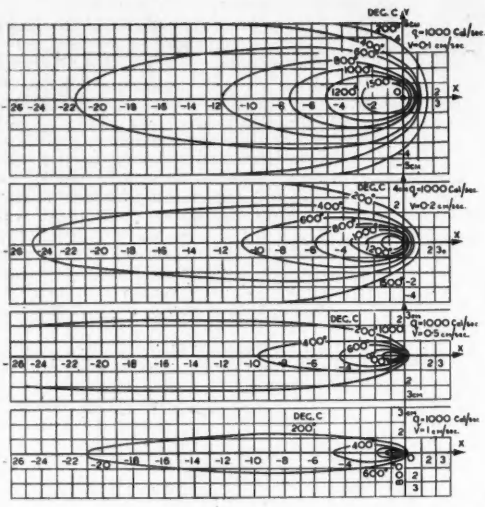

Fig. 6

The ideal cases so far considered are of value because they provide a general solution. When dealing with practical cases such as thick sheets and various rolled sections, sufficiently accurate approximations can be obtained by assuming that their surfaces form complete (or partial) barriers to the heat-flow, and that the heat, upon reaching the surface, is reflected back and " piles up " inside the infinite body. A typical example is

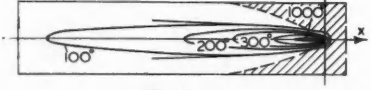

Fig. 7.

shown in Fig. 8, which concerns a thick sheet (1 cm. thick, q = 1000 Cal./sec., v = 0·1 cm./sec.). In this case three zones can be distinguished : I, similar to an infinite body, II, where a finite thickness results in considerably reduced temperatures and III, similar to a thin sheet.

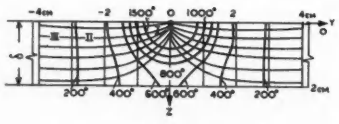

Fig. 8.

It is characteristic of all non-infinite bodies that the heated zone is deeper than in the abstract cases so far considered.

EXPERIMENTAL VERIFICATION.

Tests were carried out by the author with sheets of a thickness varying from 0·16 to 1·2 in. Temperatures were measured by means of thermocouples at points not exceeding 800 deg. C., i.e. at and beyond a distance from the centre of the arc, which varied for different experiments from 0·4 to 2½ ins.

The following tests were made :

(*a*) Butt welding for narrow strips
(*b*) Depositing a welding run on to a narrow strip
(*c*) Butt welding of plates
(*d*) Depositing a welding run on to a plate

The results agreed very well with the calculations. Fig. 9, for instance, shows the curves of temperature against time at various distances from the centre of the welding run on an 8 mm. plate. The experimental points have been plotted and the curves joining them follow very closely the theoretical curves (plain black lines).

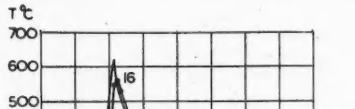

Fig. 9.

It has been found that in the regions where temperatures are below 800 deg. C. the various factors which had previously been assumed to be constant could really be taken as constant with a fair degree of accuracy as they vary only within the following limits

λ : 0·090 to 0·108 Cal./cm./sec./deg. C.
c : 1·15 to 1·3 Cal./cm.³/deg. C.
a : 0·72 to 0·092 cm.²/sec.

These are all values which correspond to about 400 deg. C., while the coefficient of heat loss from surface, α, varied from 5 to 10 × 10^{-4} corresponding to temperatures from 200 to 430 deg. C.

Thus, the applicability of the method of calculation described above, to the low temperature zones has been verified. This is the region where the predominating factor is the size, shape and cooling coefficient of the welded articles, and the method can be applied to the study of plastic deformation, recrystallization, final stage in breakdown of the austenite and the annealing effect of the heat of the arc on the hardened metal.

By inference, the method of calculation must also be regarded as sufficiently correct for the high temperature zone, where the determining factor is the speed and intensity of the arc and where it can be used as a means of studying the depth of penetration, the chemical reactions in the molten " puddle," primary and secondary crystallization of the deposited metal and the re-grouping of the crystals in the parent metal.

The knowledge thus obtained of conditions throughout the weld and the welded articles can be applied to the study and practical control of penetration, local hardening, hidden stresses and distortion effects, but this is outside the scope of the present article.

REFERENCES.

1. Lord RAYLEIGH, London, *Phil. Mag.*, Vol. 22, No. 129 Sept., 1911.
2. CARSLAW, H. S., *Introduction to the mathematical theory of the conduction of heat in solids*, London, 1921.
3. BORNEFELD, H., Doktor-Dissertation, *Technische Hochschule Berlin*, Würzburg, 1932.
4. PORTEVIN, A. and SÉFÉRIAN, D., *Chaleur et Industrie*, 1935, pp. 409-424.
5. BOULTON, N. S. and LANCE MARTIN, H. E., *Inst. Mech. Engrs. Proc.*, 1936, Vol. 133, pp. 295-348.
6. RYKALIN, N. N. *Avtógennoe Delo*, 1938, Nos. 5 and 7.
7. ROSENTHAL, D. and SCHMERBER, H., *Weld. J.*, 1941, No. 5.
8. BRUCE, W. A., *J. Appl. Physics*, 1939, pp. 578-585.
9. RYKALIN, N. N. *Prostranstvennoe raspredelenie temp. pri. dugovoi svarke*, Moskva-Leningrad, 1941.
10. RYKALIN, N. N., *Protsessy rasprostranenia tepla pri dugovoi electrosvarke, Doktor's thesis*, Moscow V.T.U., 1944.

STEAM-AIR PLANTS FOR SIMULTANEOUS PRODUCTION OF MECHANICAL ENERGY AND HEAT

By W. KARRER. (From *Bulletin Oerlikon*, Vol. 25, No. 257, October, 1945, pp. 1677-1683, 10 illustrations.)

1. INTRODUCTION.

STEAM boiler plants for the exclusive supply of heat can be converted to highly economical plants for heating and power supply by increasing the pressure and temperature at the boiler stop valve and letting the steam expand in a back-pressure turbine in producing mechanical energy. The mechanical energy which can be obtained for a given heat output is all the greater the higher the pressure and the temperature at the turbine inlet. It will be shown how by the appropriate addition of an air turbine with compressor the power available at the shaft can be approximately doubled and, in fact, with a very favourable utilisation of the additional fuel required.

2. THE BACK-PRESSURE STEAM TURBINE PLANT.

In our examination we will start with the pure heating plant (Fig. 1) in which on the grate of the boiler the heat $Q_{f\,(B)}$ of the fuel is communicated to the combustion air and the heat usefully delivered to the heat consumers h is $Q_{u\,(B)}$. The index (B) indicates that a boiler plant for the exclusive supply of heat is considered. In all the considerations which follow, to obtain a valid basis of comparison, the steam is assumed to enter the heating mains (see point h, Fig. 4) at 5 at. abs. (73·5 lbs./sq. in., abs.), and 165 deg. C. (330 deg. F.), that is slightly superheated. The condensate of the individual heat consumers is collected and heated up to nearly the temperature of evaporation in the feed-water preheater e (Fig. 1). The flue gases leave the plant at f at a temperature which is assumed to be 130 deg. C. (266 deg. F.) in all the cases considered.

In comparison with this simple plant we will now consider a back-pressure steam turbine plant (Fig. 2) with the same useful heat output $Q_{u\,(BP)} = Q_{u\,(B)}$ in the heat consumers ; at the same time, the steam turbine g yields the useful mechanical output $N_{(BP)}$. The heat $Q_{f\,(BP)}$ of the fuel which has to be introduced into the boiler exceeds $Q_{f\,(B)}$ by the heat value of this output, the heat value of the bearing friction, and the heat losses of the turbine and the mains. The combustion gases yield the heat which they absorb in the furnace gradually in the evaporator c, the superheater d and the feed-water preheater e, and leave the plant at f.

The sum of the heat value of the useful mechanical output 860 $N_{(BP)}$ and the useful heat output $Q_{u\,(BP)}$ reaches in large, modern plants about 85 per cent of the heat capacity of the fuel $Q_{f\,(BP)}$ introduced per hour. This figure is only slightly lower than the efficiency of an equivalent boiler plant without production of mechanical energy. As losses of the back-pressure turbine plant figure only the "external" losses, i.e., the radiation losses from the hot parts, the losses due to incomplete combustion, the heat carried off by the flue gases, and the friction losses in the turbine bearings, while the "internal" flow losses of the turbine are re-converted into heat and, as such, conveyed by the exhaust steam to the heat consumers ; they are, therefore, not to be debited as losses.

In the entropy diagram (Fig. 4) h represents the steam condition at the inlet to the heating mains, as established above. Starting out from this point, and considering the known dependence of the thermodynamic efficiency on the pressure of the live steam, the expansion lines for different boiler pressures have been drawn and thus the requisite superheat temperatures (points g before the turbine, points d after the superheater) determined, as well as the useful outputs $N_{(BP)}$. If the results of this investigation were summarized in an energy balance it could be seen how the part of the fuel heat, which can be converted in the back-pressure steam turbine into useful output, increases with the boiler pressure.

By comparing the sum of the heat value of the useful mechanical output 860 $N_{(BP)}$ and the useful heat output $Q_{u\,(BP)}$ with the heat $Q_{f\,(BP)}$ of the fuel used per unit of time, we obtain the overall efficiency

$$\eta_{o\,(BP)} = \frac{860\,N_{(BP)} + Q_{u\,(BP)}}{Q_{f\,(BP)}} \qquad .. \quad (1)$$

Here, N is to be introduced in kW, and Q_u and Q_f in kcal/h.

The heat balance still does not give a sufficiently

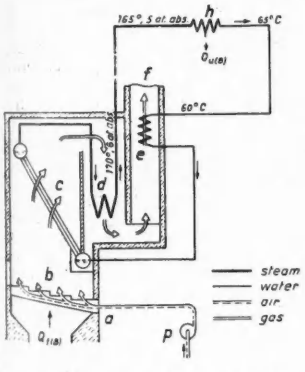

Fig. 1. **Steam boiler plant for the exclusive supply of the heat output $Q_{u\,(B)}$.**

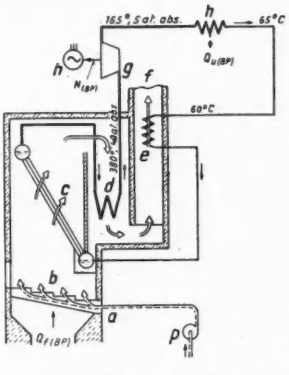

Fig. 2. **Back-pressure steam turbine plant for the supply of the useful mechanical output $N_{(BP)}$ and heat output $Q_{u\,(BP)}$.**

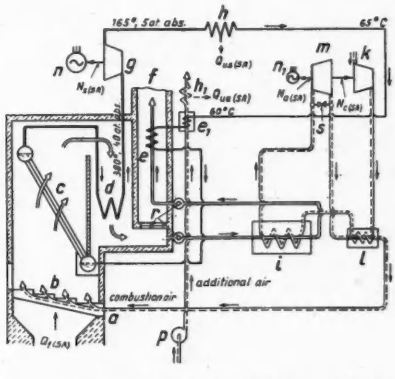

Fig. 3. **Steam-air plant for the supply of the useful mechanical outputs $N_{a\,(SA)} + N_{a\,(SA)}$ and heat outputs $Q_{ua\,(SA)} + Q_{ua\,(SA)}$.**

Legend to Figs. 1 to 3 : a = inlet of the combustion air, b = combustion chamber, c = evaporator, d = superheater, e and e_1 = feed-water preheaters, f = flue gases outlet, g = back-pressure steam turbine, h and h_1 = useful heat consumers, i = air heater, k = compressor, l = air preheater, m = air turbine, n and n_1 = generators, p = fan for combustion air, r = flue gas damper, s = regulating valve in the air circuit.

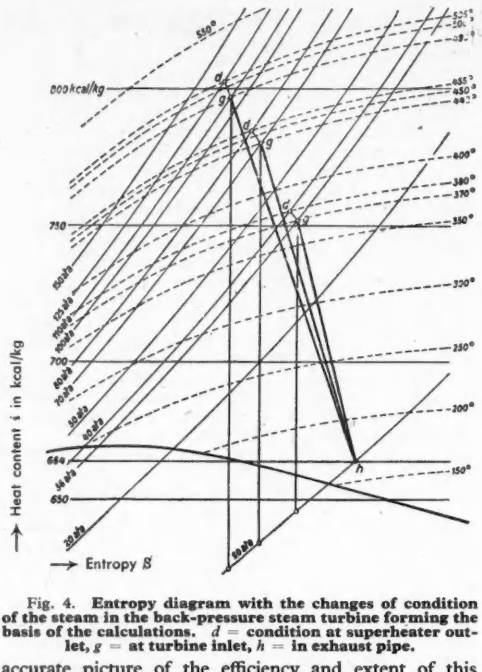

Fig. 4. **Entropy diagram with the changes of condition of the steam in the back-pressure steam turbine forming the basis of the calculations. d = condition at superheater outlet, g = at turbine inlet, h = in exhaust pipe.**

accurate picture of the efficiency and extent of this method of producing mechanical power. For this, the extra-consumption of fuel of a heating-power plant as compared with a pure heating plant of the same useful heat output must be determined, i.e., the quantity $Q_{f\,(BP)} - Q_{f\,(B)}$ in relation to the useful output $N_{(BP)}$ of the back-pressure turbine. We, accordingly, define as the *efficiency of production of mechanical power* :—

$$\eta_{(B)—(BP)} = \frac{860\ N_{(BP)}}{Q_{f\,(BP)} - Q_{f\,(B)}} \quad .. \quad (2)$$

This efficiency is round about 83 per cent in the example mentioned above, and changes but very little with the boiler pressure (Fig. 6). Furthermore, the owner of a heating plant is interested in the *amount of the energy* which the conversion of his heating plant to a heating-power plant will bring him for the same useful heat output $Q_{u\,(BP)} = Q_{u\,(B)}$. We, therefore, introduce the *quantity figure*

$$\mu_{(B)—(BP)} = \frac{860\ N_{(BP)}}{Q_{f\,(B)}} \quad .. \quad (3)$$

This characteristic figure relates to the heat $Q_{f\,(B)}$ of the fuel required for the pure heating operation in accordance with Fig. 1, because this is the only figure known to the owner of the heating plant. Decidedly clearer than μ is the specific useful output μ' in kW, which is obtainable by the conversion of the heating plant to the heating-power plant, in relation to the coal consumption in t/h of the pure heating operation before conversion. With the aid of μ our calculation yields :—

$$\mu'_{(B)—(BP)} = 1{,}165\ H_u \mu \text{ kWh/t} \quad .. \quad (4)$$

With the values of Fig. 4 and with the calorific value of the fuel $H_u = 7500$ kcal/kg, we obtain for μ' the values represented in Fig. 5. If, therefore, a pure heating plant with a coal consumption of 1 t/h is converted to a heating-power plant with a boiler pressure of 80 at. abs. (1176 lbs./sq. in., abs.), approximately 1400 kW can be raised, and as much as 1600 kW at 120 at. abs. (1764 lbs./sq. in.). Frequently, this output is too low to meet the energy demand. Instead of the pure back-pressure turbine a bleeder turbine is then installed and the energy still required generated by expansion of supplementary steam from boiler to condenser pressure. This method of generating energy, however, is very uneconomic as the heat which has to be carried away by the cooling water in the condenser is wasted.

3. THE STEAM-AIR HEATING-POWER PLANT.

By combining a back-pressure steam turbine plant as in Fig. 2, with a turbine-compressor set operating with air, for the same useful heat output a considerably greater useful mechanical output can be obtained. A possible arrangement is shown in Fig. 3. As will easily be recognized, the steam-water circuit remains externally unchanged, only the feed-water preheater is divided with advantage in two apparatus e and e_1 in tandem on the water side. The combustion air arrives preheated under the grate b ; the flue gases heat in succession the evaporater c, the superheater d, the air heater i and the feed-water preheater e, and leave the plant at f at the temperature of 130 deg. C. (266 deg. F.) assumed in the former examples (Figs. 1 and 2). The air compressor k draws in air from outside, compresses it while absorbing the driving output $N_{e(SA)}$ and delivers it through the air preheater l and the air heater i to the air turbine m where it expands almost down to atmospheric pressure in yielding the useful output $N_{a(SA)}$ to the generator n_1 and the driving output $N_{e(SA)}$ to the compressor k. The still hot air then flows through the preheater l giving up heat to the compressed air from k. Part of it then arrives as combustion air under the grate of the boiler, while the rest proceeds as additional air to the feed-water preheater e_1 and the heating apparatus h_1, where it yields the useful heat output $Q_{ua(SA)}$. Using the notation of Fig. 3, the total useful mechanical output of the steam-air plant can be expressed as follows :—

$$N_{(SA)} = N_{s(SA)} + N_{a(SA)} \quad .. \quad (5)$$

In an analogous manner, the available useful heat output is :—

$$Q_{u(SA)} = Q_{us(SA)} + Q_{ua(SA)} \quad .. \quad (6)$$

If the air turbine plant is designed only for the quantity of air required for combustion by the steam boiler, the losses of the back-pressure steam turbine plant are increased only by the external losses of the air system, i.e. the losses by radiation from the hot parts and the losses by friction in the bearings of the air turbine and compressor. The overall efficiency therefore is only slightly lower than with a back-pressure steam turbine plant as Fig. 2. If the air turbine plant is designed for a larger quantity of air, its useful output $N_{a(SA)}$ rises with only a slight decrease in the overall efficiency, provided that the available heat in the extra air can be fully utilized.

To enable a judgement to be formed of the efficiency and the ratio of conversion of the useful mechanical energy from the heat available in the fuel of a pure heating plant of the same useful heat output, we will establish for the steam-air plant the analogous relation as for the back-pressure steam turbine plant : the efficiency of production of mechanical power in relation to the increased consumption of fuel required for it in comparison with a pure heating plant is :—

$$\eta_{(B)—(SA)} = \frac{860\ N_{(SA)}}{Q_{f(SA)} - Q_{f(B)}} \quad .. \quad (7)$$

For the quantity figure, referred to the heat of fuel of the pure heating plant, we obtain :—

$$\mu_{(B)—(SA)} = \frac{860\ N_{(SA)}}{Q_{f(B)}} \quad .. \quad (8)$$

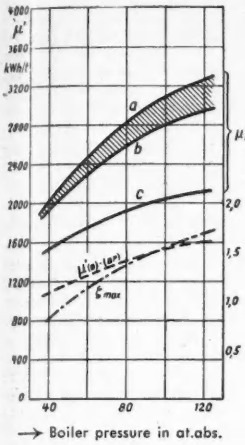

→ Boiler pressure in at.abs.

Fig. 5. **If a heating plant according to Fig. 1, consuming 1 ton of coal per hour, is converted to a back-pressure steam turbine plant as per Fig. 2 or a steam-air plant as per Fig. 3, μ' kW can be gained. ζ_{max} = highest possible quantity ratio of the steam-air plant.**

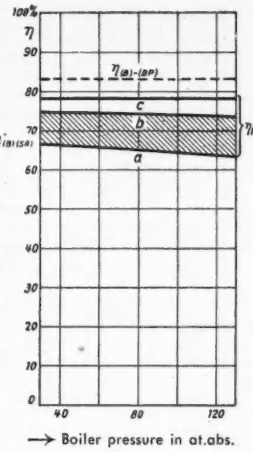

→ Boiler pressure in at.abs.

Fig. 6. **Efficiency of production of mechanical power in reference to the extra demand of heat of fuel compared with a pure heating plant of equal output as a function of the boiler pressure.**

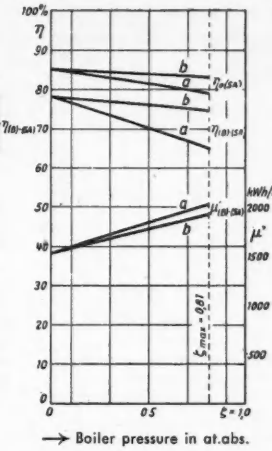

→ Boiler pressure in at.abs.

Fig. 7. **Efficiencies (as Fig. 6) and useful mechanical outputs (as Fig. 5) at a boiler pressure of 40 at. abs. (588 lbs./sq. in.) and 380 deg. C. (716 deg. F.) as a function of the quantity ratio ζ.**

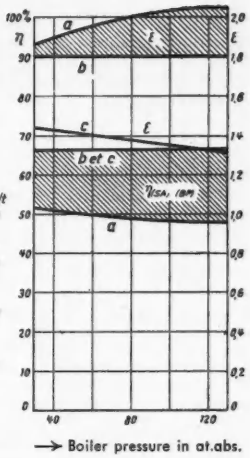

→ Boiler pressure in at.abs.

Fig. 8. **Ratio ϵ of the useful mechanical output of a steam-air plant to that of a back-pressure steam turbine plant of equal useful heating output. Efficiency $\eta_{(SA)-(BP)}$ for the gain in mechanical output to be obtained with a steam-air plant as compared with a back-pressure steam turbine plant, in reference to the corresponding extra consumption of fuel heat.**

Legend to Figs. 5 to 8: Lines in full: Steam-air plant. Broken lines: Back-pressure steam turbine plant. *a* and *b* = operation with the maximum quantity of extra air, *a* without utilization of the waste heat of the extra air, *b* with full utilization. *c* = operation without extra air.

For the specific useful output, referred to the coal consumption of 1 t/h of the pure heating plant (before conversion), we have to put :—

$$\mu'_{(B)-(SA)} = 1{,}165\, H_u\, \mu_{(B)-(SA)} \text{ kWh/t} \quad .. \quad (8a)$$

Finally, the overall efficiency is :—

$$\eta_{o(SA)} = \frac{860\, N_{(SA)} + Q_{u(SA)}}{Q_{f(SA)}} \quad .. \quad (9)$$

In these equations the mechanical outputs N must again be inserted in kW and the heating outputs Q in kcal/h.

In the steam-air plant, the quantity ratio ζ between the extra air and the combustion air occurs as a new variable. This ratio has to be adapted to the demand for mechanical power and heat from case to case. If for the steam turbine we fix the condition at the outlet, at $p = 5$ at.abs. (73·5 lbs./sq. in., abs.), $t = 165$ deg. C. (330 deg. F.) as before, and the boiler pressure at 40 at. abs. (588 lbs./sq. in., abs.), we obtain the variation of the characteristic quantities in relation to the ratio of the quantity of air ζ, as shown in Fig. 7. This ratio cannot be selected at random. Its highest value is given by the differences in temperature in the air heater *i* which are necessary for the heat exchange to take place with heating surfaces of economically justifiable size ; in the present case, $\zeta_{max} = 0{\cdot}81$. Fig. 7 presents the values of η and μ' for the two limiting cases with full and with no utilization of the waste heat available in the extra air.

For the estimation of the advantages offered by a steam-air plant, we again start out from a pure heating plant as per Fig. 1, in which 1 ton of coal, and consequently the quantity of heat $Q_{f(B)}$, is fed into the boiler per hour and the useful heat output $Q_{u(B)}$ is obtained. By installing a back-pressure steam turbine and raising the boiler pressure from 6 to 40 at. abs. (88 to 588 lbs./sq. in., abs.), Fig. 2, with the greater heat $Q_{f(BP)}$ of the fuel the mechanical output $N_{(BP)} = \mu'$ is gained in addition to the same heat output $Q_{u(BP)} = Q_{u(B)}$, and in accordance with Fig. 5 amounts to 1070 kW. If a conversion is made instead according to Fig. 3, i.e. a steam-air plant of the same useful heat output is installed, then, as will be seen from the values of μ' in Fig. 7, 1540 to 2030 kW can be produced depending on the quantity of additional air. Thereby the efficiency $\eta_{(B)-(SA)}$, referred to the extra consumption of fuel heat in comparison with the pure heating operation, which in a back-pressure steam turbine plant was found to be 83 per cent, attains the remarkably high figure of 78 per cent for operation without extra air ($\zeta = 0$) ; with increasing quantities of extra air it falls to 75 and 65 per cent according to the degree of utilization of the waste heat contained in the extra air.

With the higher boiler pressure, as Fig. 5 shows, the maximum possible ratio of the extra air to the combustion air ζ_{max} and the available mechanical output μ' per 1 t/h of coal consumed by the pure heating plant before conversion increase. Three cases are to be distinguished here : (a) Operation with the maximum possible quantity of extra air (ζ_{max}), but without utilization of the heat available in the extra air ; (b) operation as under (a), but with full utilization of the heat of the extra air ; (c) operation without extra air. The mode of operation (a) yields the greatest mechanical output ; with a boiler pressure of 120 at. (1764 lbs./sq. in.) it reaches 3230 kWh per 1 ton of coal consumed by the heating plant compared, whereas the back-pressure steam turbine under otherwise equal conditions gives an output of 1620 kWh, only about one-half. It is true that the efficiency is comparatively low (see Fig. 6). It drops, with this method of operation, from 66 per cent (at a boiler pressure of 40 at. abs.) to 63·5 per cent (at 120 at.), but is still far above the highest efficiencies of large self-contained thermal power plants.

The advantages described often render the conversion in steam-air plants, not only of boiler plants but also back-pressure steam turbine plants, economically advantageous. In the second case, the ratio of the possible increase in output $\epsilon = N_{(SA)}/N_{(BP)}$ for the different methods of operation with or without extra air and with full or no utilization of the heat available in the extra air is of interest. This information is contained in Fig. 8

which also shows the variation of the efficiency for the gain in mechanical output to be obtained with a steam-air plant as compared with a back-pressure steam turbine plant, in relation to the corresponding extra consumption of fuel heat :—

$$\eta_{(SA)-(BP)} = \frac{N_{(SA)} - N_{(BP)}}{Q_{(SA)} - Q_{(BP)}}$$

This efficiency naturally is somewhat lower than that calculated above from equation (7) ; it presents, nevertheless, considerable interest, especially in the two cases (b) and (c) (66·5 per cent) ; but even in case (a) it is not nearly reached in any self-contained thermal power plant.

4. THE REGULATION OF THE PRODUCTION OF MECHANICAL OUTPUT AND HEAT OUTPUT.

As with every back-pressure steam turbine, with the steam-air plant either the heating output must be adjusted to the heat demand of the consumers, then the mechanical power generated has to be absorbed by a large electrical network with which the generators run in parallel ; or the output of mechanical power must be adjusted to the energy demand of the consumers, and the heat output be disposed of. In the first case, the adjustment to a reduced heat demand is effected in the same way as with the back-pressure plant, i.e. by throttling the supply of steam and air (combustion air and extra air). With part load, the efficiencies decrease in the same way as with the back-pressure plant. Beside this regulation by throttling there are fundamentally two further possibilities :—

With decreasing heat demand only the steam side is throttled by reducing the supply of combustion air to the boiler, and of steam to the steam turbine, while the quantities of the air side remain unaltered, until finally, in the theoretical limiting case, the steam production would drop to nought and all the heat of the fuel be transferred in the air heater to the pressure air. The whole arrangement would then operate as a pure air turbine plant. As the limit of efficiency for the production of mechanical power with the steam plant shut down and with no utilization of the waste heat, a value of 25 to 30 per cent would be obtained. To reach this limiting case special measures would, of course, have to be adopted. Such a regulation, with decreasing heat demand, enables *the production of the mechanical power to be maintained in a much higher degree than the regulation of a back-pressure steam turbine plant by pure throttling.*

The second possibility, with decreasing power demand, consists in first throttling only the air side by reducing step by step the extra air to nought and then in throttling further the air flowing through the compressor and air turbine, while the air required for combustion is passed direct into the boiler by means of a special fan *p* (Fig. 3). With this regulation pure back-pressure operation is reached step by step and, *with a falling demand for mechanical power, the useful heat output can be kept constant over a wide range.*

For regulating the output on the air side all known methods of regulation for gas turbines can be applied, e.g. by-passing the air turbine *m* by a regulating valve *s* (Fig. 3), temperature regulation, speed variation ; also pressure gauge regulation on the air side with closed-circuit is possible, provided a heat exchanger is installed for the transfer of the waste heat of the air plant to the combustion air of the boiler.

In all these processes the quick acting regulation of the air side by the centrifugal governor of the air turbine, and the more slowly acting regulation of the steam boiler to constant pressure at the steam turbine are independent of each other as the quantity of the combustion air to the boiler can be adjusted independent of the air side.

RUSSIA

INFLUENCE OF THE SPEED OF DEFORMATION UPON THE RESISTANCE OF METALS TO PLASTIC DEFORMATION

By L. D. Sokolov. (From *Journal of Technical Physics*, Vol. 16, No. 4, 1946, pp. 437-441, 5 illustrations.)

The materials investigated were lead, copper, and various steels of the following analyses :—

	Steel No. 3	Steel No. 5	Steel U-10.
C, per cent	0·17	0·56	1·08
Mn, per cent	0·46	0·72	0·28
Si, per cent	0·17	0·20	0·32
P, per cent	0·028	0·026	0·04
S, per cent	0·04	0·036	0·03

The test pieces were 10 mm. in diameter and 20 mm. long. They were compressed in a 30 ton Amsler machine at average speeds of 0·01 mm. per second and of 1 mm. per second. Compression tests were also made with a Charpy 15 kg. machine specially equipped for this purpose. As the blows of the Charpy pendulum were delivered from various elevations, the initial impact speed varied from 1,700 to 5,200 mm. per second. By taking the final impact speed as zero, the mean impact speed was assumed to be the arithmetic mean which ranged from 850 to 2,600 mm. per second. As will be shown below, at the high speeds employed the variation in speed proved to be practically without influence upon the stress ; and the speed in the dynamic test was therefore taken as 2000 mm. per second.

In the case of the tests conducted with the Charpy machine, the specimens were heated first in an electric muffle furnace and then either in a nichrome resistance furnace or in an electric furnace with platinum tube arranged close to the Charpy machine. The heating temperatures used, in the case of the copper specimens,

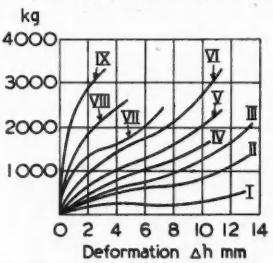

Fig. 1. **Deformation diagrams for No. 3 steel.**

I — 1100 deg. C., speed 0·01 mm./sec.
II — 900 „ „ „ 0·01 „ „
III — 100 „ „ „ 1 „ „
IV — 700 „ „ „ 0·01 „ „
V — 900 „ „ „ 1 „ „
VI — 700 „ „ „ 1 „ „
VII — 1100 „ „ „ 2,000 „ „
VIII — 900 „ „ „ 2,000 „ „
IX — 700 „ „ „ 2,000 „ „

were 500, 700, and 900 deg. C. ; and in the case of the steel specimens 700, 900, and 1,100 deg. C. The temperatures were measured by means of a platinum-platinum rhodium couple which was pressed against the specimen. The test pieces were held at the given temperature for 15-20 minutes and then quickly removed from the furnace and mounted for testing. The time between removing the specimen from the furnace and

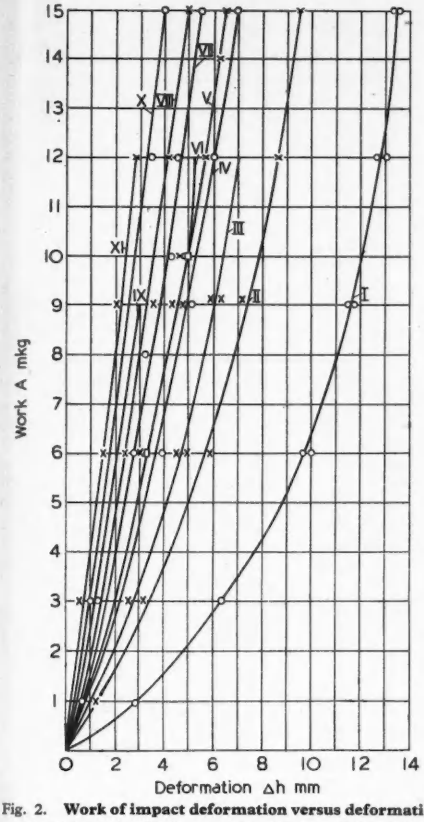

Fig. 2. **Work of impact deformation versus deformation.**
I, Lead at 20 deg. C.; II, Copper at 900 deg. C.; III, Steel No. 3 at 1,100 deg. C.; IV, Steel No. 5 at 1,100 deg. C.; VI, Steel No. 3 at 900 deg. C.; VII, Copper at 500 deg. C.; VIII, Steel No. 5 at 900 deg. C.; IX, Steel No. 3 at 700 deg. C.; X, Copper at 20 deg. C.; XI, Steel No. 5 at 700 deg. C.

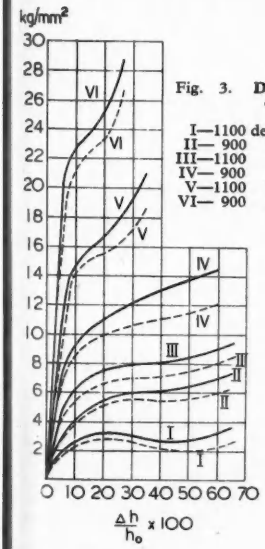

Fig. 3. **Deformation characteristics of No. 3 steel.**

I—1100	deg. C.,	speed	0·01	mm./sec.	
II— 900	,,	,,	0·01	,,	,,
III—1100	,,	,,	1	,,	,,
IV— 900	,,	,,	1	,,	,,
V—1100	,,	,,	2,000	,,	,,
VI— 900	,,	,,	2,000	,,	,,

subjecting it to the impact-compression test was 3-5 seconds, which resulted in a drop in metal temperature from 15-20 deg. C. according to the initial temperature. This temperature drop was compensated for by a corresponding higher initial temperature. In the case of the Amsler machine arrangements were also made for heating the test piece in place. In the static tests the speed of compression was determined as $v = \Delta h/t$. Automatic indicator diagrams were taken during the compression process proper ; these were evaluated and compression speed *versus* deformation diagrams charted. A few

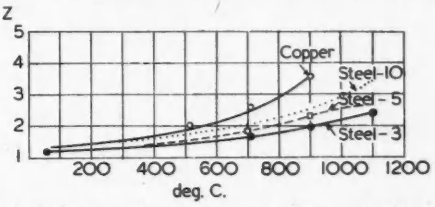

Fig. 4. **Influence of temperature upon the speed-of-deformation coefficient for v_0 = 0·01 mm./sec. and v_1 = 1 mm./sec.**

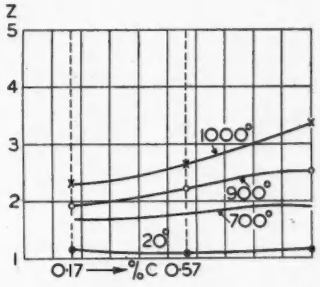

Fig. 5. **Influence of carbon percentage upon the speed-of-deformation coefficient for v_0 = 0·01 mm/sec. and v_1 = 1 mm./sec.**

typical indicator diagrams are shown in Fig. 1. Each test was repeated from two to five times.

The results obtained with the Charpy machine are plotted in Fig. 2. Both in the static and in the dynamic tests the specific pressure p was determined from $p = P/F$, where, in the case of impact tests, $P = dA/dh$. The true stress s was found from Unksov's formula

$$p = 2s\left(\frac{h}{\mu d}\right)^2\left(e^{\frac{\mu d}{h}} - 1 - \frac{\mu d}{h}\right)$$

where μ is the coefficient of friction between the engaged surfaces of specimen and machine. The following values for the friction coefficient were taken from existing literature on the subject :—

Copper at high temperature	..	..	0·25
Copper at room temperature	..	..	0·30
Steel at high temperature	..	..	0·35
Steel at room temperature	..	..	0·30

TABLE I.

Temperature deg. C.	Coefficient	Lead	Copper	Steel No. 3	Steel No. 5	Steel No. U-10
20	100	2·07	1·17	1·16	1·10	1·075
20	2,000	1·48	1·35	1·35	1·50	—
500	100	—	1·95	—	—	—
500	2,000	—	2·20	—	—	—
700	100	—	2·36	1·70	1·88	1·87
700	2,000	—	2·68	2·0	1·985	2·10
900	100	—	3·54	1·87	2·26	2·38
900	2,000	—	2·90	2·24	2·44	2·80
1,100	100	—	—	2·32	2·60	3·50
1,100	2,000	—	—	2·22	2·68	3·22

Specific pressures and true stresses as obtained under various test conditions are charted in Fig. 3. The influence of the deformation speed upon the magnitude of the true stress can be established by comparing the ratio $\psi = v/v_o$ with the ratio $Z = s/s_o$, where v and s are the highest speed of deformation and its correlated stress, and v_o and s_o are the lowest speed of deformation and its correlated true stress. In this way the speed-of-deformation coefficient Z will serve to show the extent to which the true stress is increased if the deformation speed is increased ψ times. Values for Z are given in Table I.

These values for Z are charted as function of the temperature in Fig. 4, while the relationship between Z and the carbon percentage of the steel specimens is plotted in Fig. 5 for different temperatures.

From these data it can be concluded that :—

1. The coefficient Z increases with the temperature.
2. The coefficient Z increases with the carbon content of the steel at high temperature, this increase being the greater the higher the temperature.
3. The coefficient Z falls very slightly with increasing carbon percentage at 20 deg. C.
4. At a given temperature the value for Z depends upon the melting point of the metal and it increases greatly with a lower melting point.
5. The influence of the deformation speed upon the stress decreases sharply with the speed.
6. The steepness of the deformability characteristic (deformation *versus* true stress, Fig. 3) increases with rising speed and with falling temperature.

RUSSIA

REGIONAL HOT-WATER SUPPLY

By B. SHIFRINSON, M. ZAKS, C. KOPIEV, and M. PIK. (From *Promishlennaya Energetika*, No. 2, 1946, pp. 6-8 and 9-10, 4 illustrations.)

GENERALLY, the initial water temperature for district heating should be as high as possible. 130 deg. C. is commonly regarded as a standard, but there is no real need for this limitation and greater economy can be achieved if this figure is exceeded ; 150 deg. C. or even 180 deg. C. is quite feasible, particularly if the load is mainly industrial.

On the other hand, the selection of a suitable return-water temperature is difficult, depending on the way in which the water is utilized or rather, on the proportion of the various kinds of loading. Low return-water temperature means higher heat extraction, and therefore lower cost per heat unit to the supplier, but greater initial cost of users' installations. Thus, if the mains are long and relatively expensive, the temperature of the return water should be low ; the same applies if the heat is extracted in air heaters which are cheap and efficient. If, on the other hand, the mains have to supply a great number of domestic installations of the " no pressure " type requiring special and expensive devices against boiling, then it pays to return the water at a higher temperature. About 70 deg. C. is regarded as an average, but the final choice should always be made in accordance with working conditions.

The articles under review, give a great number of formulæ and nomograms for the calculation of both initial and final temperatures. They are based on Russian costs and cannot, therefore, be applied directly to the planning of installations in this country ; but the authors' method of the theoretical analysis is unique in its detailed thoroughness and should prove to be of great interest to specialists on this subject.

REGULATION OF HEAT SUPPLY TO INDIVIDUAL BOILERS.

In regional heating installations, the hot-water demand of individual consumers is characterized by daily and seasonal fluctuations. A demand on a round-the-clock basis would result in higher thermal efficiency and reduced first cost, but naturally there is a great tendency to make use of the hot-water supply during the day-time only. The systems are usually arranged in such a manner that, if mains water is cut off from consumers' boilers, it is merely by-passed into central heating pipes, resulting in but a slight reduction in heat consumption.

Observations made at central power plants No. 2 and 3 at Leningrad showed that cutting off the entire domestic load, representing 25 per cent of the total, could not be detected on the power plant instruments. In other words, the water that might have been saved, simply found another use for itself in the circulating systems of industrial consumers.

This difficulty makes it next to impossible to regulate the water supply economically at the source, neither can worth-while economies be effected by local regulation of flow in strict accordance with hourly requirements. It was, therefore, proposed in Leningrad to " regulate by not regulating " as it were, i.e. to set the flow through the boilers of the principal consumers to a constant value, as calculated by means of a diaphragm and to leave it so adjusted for the whole season. When this was put to the test in two big installations (public baths), heat consumption of the whole district was reduced to a greater extent than was previously thought possible, even more than by resorting to a reduction in mains water temperature below specification value.

Admittedly, this method of operation also allows a certain amount of heat to go to waste, since, at times when the consumer is not using much hot water, the return water in the mains is unnecessarily hot but the resulting losses are by far outweighed by the benefits obtained through steady operation.

In the case of systems in which the mains temperature does not exceed 100 deg. C., this type of control is applicable to all installations and no modifications are required. But if the mains contain water of a higher temperature, the absence of regulators may result in the boiling of the secondary water, and, in many cases, may thus create a dangerous condition.

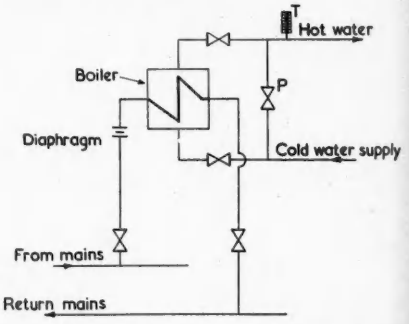

In such cases it is necessary to control the temperature of the secondary water, as shown diagramatically in the accompanying illustration. When by-passing cold water in required quantities through P, controlled by the thermostat at T, the temperature of consumers' water can be kept at whatever figure is considered safe and desirable.